4D printed shape-shifting biomaterials for tissue engineering and regenerative medicine applications

Kalogeropoulou, Maria; Díaz-Payno, Pedro J.; Mirzaali, Mohammad J.; van Osch, Gerjo J.V.M.; Fratila-Apachitei, Lidy E.; Zadpoor, Amir A.

DOI
10.1088/1758-5090/ad1e6f

Publication date
2024

Document Version
Final published version

Published in
Biofabrication

TOPICAL REVIEW • OPEN ACCESS

4D printed shape-shifting biomaterials for tissue engineering and regenerative medicine applications

Biofabrication

TOPICAL REVIEW

4D printed shape-shifting biomaterials for tissue engineering and regenerative medicine applications

Maria Kalogeropoulou[1,5], Pedro J Díaz-Payno[1,2,5,*], Mohammad J Mirzaali[1], Gerjo J V M van Osch[1,2,3], Lidy E Fratila-Apachitei[1] and Amir A Zadpoor[1,4,*]

[1] Department of Biomechanical Engineering, Faculty of Mechanical Engineering, Delft University of Technology, Delft, CD 2628, The Netherlands
[2] Department of Orthopedics and Sports Medicine, Erasmus MC University Medical Center, 3015 CN Rotterdam, The Netherlands
[3] Department of Otorhinolaryngology, Head and Neck Surgery, Erasmus MC University Medical Center, 3015 CN Rotterdam, The Netherlands
[4] Department of Orthopedics, Leiden University Medical Center, Leiden, The Netherlands
[5] The authors contributed equally to this work.
[*] Authors to whom any correspondence should be addressed.

E-mail: pedrojose.diaz@imdeamaterials.org and a.a.zadpoor@tudelft.nl

Keywords: shape-change transformation, regenerative medicine, 3D printing, shape-shifting, stimuli-responsive, smart materials

OPEN ACCESS

RECEIVED
30 August 2023

REVISED
12 December 2023

ACCEPTED FOR PUBLICATION
15 January 2024

PUBLISHED
9 February 2024

Abstract

The existing 3D printing methods exhibit certain fabrication-dependent limitations for printing curved constructs that are relevant for many tissues. Four-dimensional (4D) printing is an emerging technology that is expected to revolutionize the field of tissue engineering and regenerative medicine (TERM). 4D printing is based on 3D printing, featuring the introduction of time as the fourth dimension, in which there is a transition from a 3D printed scaffold to a new, distinct, and stable state, upon the application of one or more stimuli. Here, we present an overview of the current developments of the 4D printing technology for TERM, with a focus on approaches to achieve temporal changes of the shape of the printed constructs that would enable biofabrication of highly complex structures. To this aim, the printing methods, types of stimuli, shape-shifting mechanisms, and cell-incorporation strategies are critically reviewed. Furthermore, the challenges of this very recent biofabrication technology as well as the future research directions are discussed. Our findings show that the most common printing methods so far are stereolithography (SLA) and extrusion bioprinting, followed by fused deposition modelling, while the shape-shifting mechanisms used for TERM applications are shape-memory and differential swelling for 4D printing and 4D bioprinting, respectively. For shape-memory mechanism, there is a high prevalence of synthetic materials, such as polylactic acid (PLA), poly(glycerol dodecanoate) acrylate (PGDA), or polyurethanes. On the other hand, different acrylate combinations of alginate, hyaluronan, or gelatin have been used for differential swelling-based 4D transformations. TERM applications include bone, vascular, and cardiac tissues as the main target of the 4D (bio)printing technology. The field has great potential for further development by considering the combination of multiple stimuli, the use of a wider range of 4D techniques, and the implementation of computational-assisted strategies.

1. Introduction

There is a rising interest in engineering tissues to closely mimic the physiological structure and the composition of their native counterparts, so that they can be used for the repair or regeneration of damaged tissues as well as for the development of highly reliable *in vitro* disease models. Most tissue engineering approaches use scaffolds, which are matrices supporting cell attachment, proliferation, and extracellular matrix deposition [1, 2]. Most common conventional techniques for scaffold fabrication include solvent-casting particulate leaching [3], gas foaming [4], fiber bonding [5], melt molding

[6], freeze-drying [7, 8], and solution casting [9]. However, these techniques lack sufficient control over the internal geometry of the scaffold, as well as the tailored distribution and interconnectivity of pores in the scaffolds.

These challenges have been partially addressed by the introduction of three-dimensional (3D) printing, which enables the fabrication of sophisticated, patient-specific, and biomimetic constructs with precise spatial control over the material-forming scaffold in a layer-by-layer and reproducible manner. Common 3D printing methods for tissue engineering and regenerative medicine (TERM) applications include material extrusion (ME), material jetting (MJ), powder bed fusion (PBF) and vat photopolymerization (VP). A detailed overview of the working principles as well as the applications of the biofabrication techniques can be found elsewhere [10–12]. Printing using cell-laden biomaterials, also known as *bioinks*, is collectively referred to as (*3D*) *bioprinting*. Bioprinting has had some level of success in the fabrication of several tissue types *in vitro*, including muscle [13], cartilage [14], bone [15], skin [16], vasculature [17], and neuronal tissue [18].

While 3D printing is a promising biofabrication method, it has significant limitations in the engineering of complex out-of-plane features and shapes, and in achieving temporal variations of the properties of multi-material constructs [19]. These limitations are particularly evident in the fabrication of tubular or curved living structures [20], which usually requires the use of sacrificial materials and supports [21], introducing additional post-printing processing steps and, thus, increasing the total fabrication time [19, 22]. For instance, using one of the available 3D printing approaches, such as ME, to fabricate multi-material, curved and porous scaffolds would require a significant number of print-head changes, for sacrificial material, as well as complex design and coding. Moreover, optimal tissue formation may require temporal changes in the geometry and other properties of the scaffold. These spatial and temporal complexities can be best addressed with four-dimensional (4D = 3D + time) printing as the next generation of biofabrication technologies.

Four-dimensional printing combines the same fabrication principles as 3D printing with the use of stimuli-responsive biomaterials while introducing a post-printing phase. During this phase, the application of one or more stimuli triggers a transformation of the printed structure, inducing either a structural or a functional change in the construct. The term 4D printing was coined in 2013 by Skylar Tibbits, the director and founder of the Self-Assembly Lab (MIT), who demonstrated the humidity-induced self-assembly of 3D printed structures into complex shapes [23]. In another early study, Sydney Gladman *et al* developed a biomimetic hydrogel composite ink from cellulose fibrils embedded in an acrylamide matrix, and used it to 3D print complex, plant-inspired structures that could self-transform into 'flowers' upon immersion in water [24]. In this way, 4D printing simplifies the fabrication of curved or tubular structures by using a rectangular bilayer which, upon proper stimulation, self-rolls into a tube or a dome-like structure [25–28]. Furthermore, the combination of 4D printing and shape-memory polymers enables the fabrication of constructs that can be compressed to smaller sizes, to allow their implantation through minimally invasive procedures, and which could regain their original or predesigned size and shape upon reaching the defect site [29].

As 4D printing is gaining momentum, different definitions have arisen. For instance, gradual degradation of 3D printed scaffolds [30] as well as maturation of 3D printed tissues [31] have been considered a type of 4D printing, due to their time-dependency. Furthermore, a functional change of the scaffold, that is not accompanied by a shape-change, has been suggested as an additional dimension to 3D printing, such as controlled enzyme-mediated processes or supramolecular tuning of cell-hydrogel interactions [32, 33]. In this review, we adopt the definition of Tibbits and regard the fourth-dimension as '*the transformation over time, emphasizing that printed structures are no longer simply static, dead objects; rather, they are programmably active and can transform independently.*' [23]

Earlier attempts to summarize the advances of 4D printing have been made [31, 34, 35]. However, the swift development of the field requires an equally updated overview. This review aims to highlight the developments of the technology for achieving controlled shape-changing of constructs for TERM applications. Toward this aim, the printing methods, the stimuli, the shape-changing mechanisms as well as the cell incorporation strategies are reviewed and discussed. Finally, future research directions and perspectives of 4D (bio)printing for TERM applications are proposed.

2. Search method and general output

Four databases were used to search for 4D printing articles: Pubmed, Scopus, Research Gate and Google Scholar. The following keywords were used: '4d bioprinting' OR '4d printing' AND 'shape memory' OR 'shape changing' OR 'shape shifting' OR 'shape morphing' OR 'self folding' OR 'stimuli responsive' OR 'self assembling' AND 'tissue', and the title of the papers was selected as the search field. Of the 374 papers that were returned, 39 review papers were excluded. Of the 335 remaining studies, 256 were excluded from abstract screening as irrelevant to the subject of 4D printing and/or TERM. Reviewing of the 79 remaining papers resulted in the further exclusion of 55 studies that were either focusing on the development of a 4D printed medical device or on a

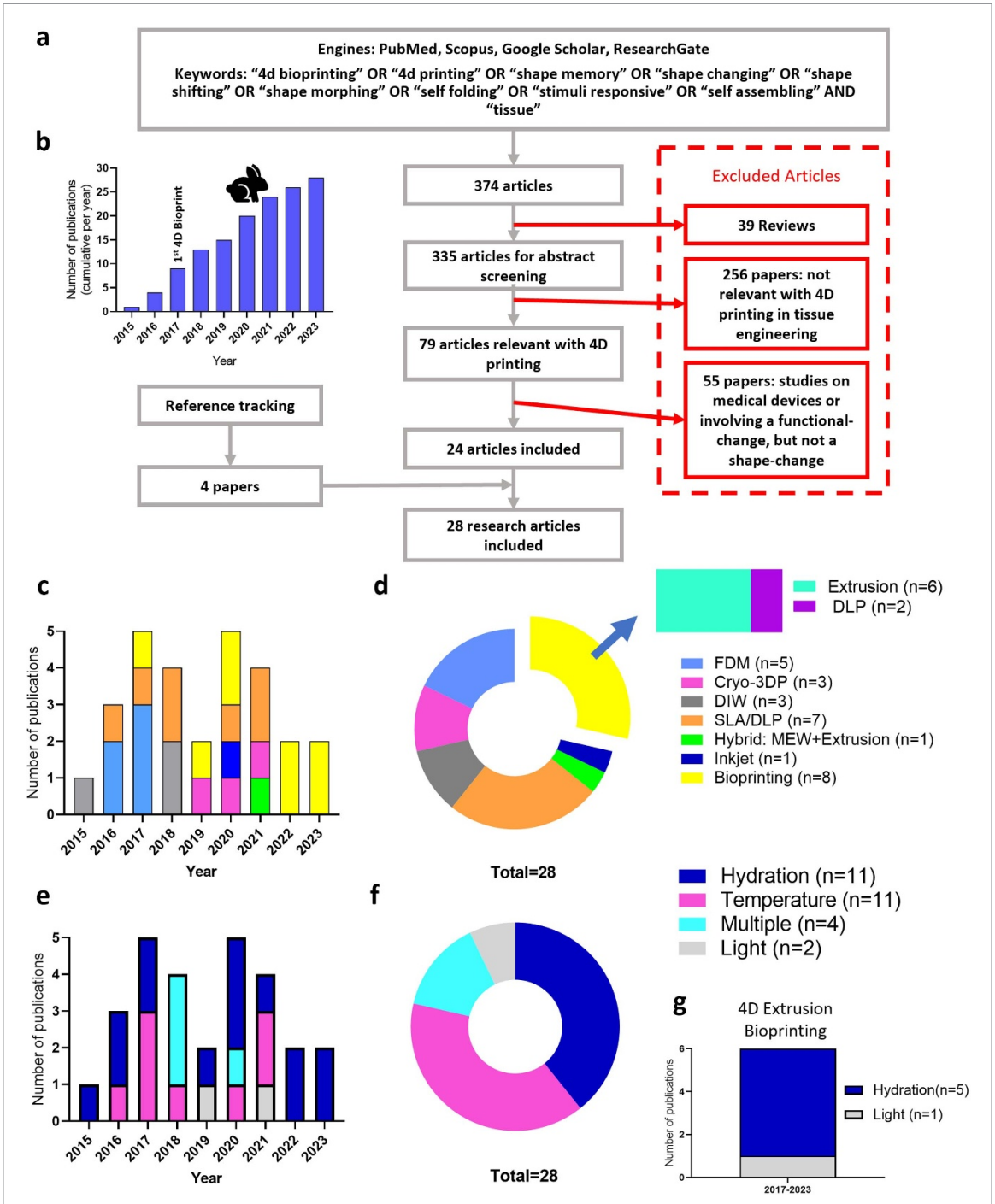

Figure 1. A schematic representation of the search strategy and results. (a) A flowchart depicting the filtering procedure for acquiring the reviewed papers focused on shape-change 4D printing for TERM applications. (b) The distribution of the included research papers per year of publication highlighting the first 4D bioprinting study in 2017 and the first *in vivo* study using a rabbit model for trachea regeneration. (c) The distribution of the reviewed studies according to their fabrication method and year (with part of 2023). (d) The distribution of the reviewed studies according to the applied 4D printing (pie chart) or 4D bioprinting technique (rectangular chart). (e) The distribution of the articles per stimulus and per year. (f) A pie chart showing the distribution of papers for each of the stimuli. (g) The distribution of 4D bioprinting studies according to their stimulus type and publication year. n: number of articles included in each category.

functional rather than a spatial change of the printed structure. Furthermore, reference tracking of the included studies lead to the inclusion of four more articles. Finally, 28 papers were considered suitable for the present review. As 4D printing is a relatively new technology, all the included studies were published between 2015 and 2023 and, thus, no time filtering was necessary. The selection procedure as well as the distribution of the papers per publication year are summarized in figure 1(a). The first 4D study in which cells were bioprinted was in 2017, and the first *in vivo* study was in 2020 in a rabbit model (figure 1(b)). The main target journals are mainly focused on the biofabrication and materials fields.

4D printing-based shape-shifting scaffolds are fabricated with 3D printing techniques and are, subsequently, exposed to one or more external stimuli that trigger their shape transformation. The techniques used in 4D studies include extrusion-based approaches (e.g. fused deposition modelling (FDM)), cryogenic 3D printing (cryo-3DP), direct ink writing (DIW)), stereolithography (SLA), digital light processing (DLP), melt-electrowritting (MEW), and inkjet printing (figures 1(c) and (d)). Unlike conventional 3D printing techniques, bioprinting methods use a modified technical approach that is compatible with the deposition of living cells. The distribution of the studies per year based on the fabrication technique used demonstrates that 4D bioprinting has recently become more relevant (figure 1(c)). From the previously mentioned techniques, only extrusion-based techniques and DLP have been used in studies implementing a shape-shifting 4D bioprinting approach for TERM applications (figure 1(d)).

Shape transformation in 4D (bio)printed scaffolds is triggered by the application of one or more stimuli, post-fabrication. The reported stimuli include hydration, temperature, and light, as well as multiple stimuli with the most studied being temperature and hydration (figures 1(e) and (f)). In particular, hydration is noted to be almost exclusively used as stimulus for 4D bioprinting studies in the last years (figure 1(g)).

3. Printing methods for shape-shifting scaffolds

The following sections describe each of the techniques used in the reviewed article (table 1).

3.1. Extrusion-based

3.1.1. FDM

FDM has become the most widespread 3D printing technique after it was first introduced in the late 1980s [36]. During the printing process, a thermoplastic polymer in powder or filament form is introduced to the heating chamber of the device and is melted (figure 2(a)). Subsequently, the molten polymer is extruded from the nozzle and deposited layer-by-layer on the printing surface to create a scaffold [37]. Hendrikson *et al* used FDM to fabricate scaffolds using shape-memory polyurethane [38]. Interestingly, the authors observed that the recovery of the shape of the compressed scaffolds back to its original state resulted in the elongation of mesenchymal stem cells (MSCs) seeded on the structure post-printing, thus demonstrating that even a single mechanical stimulus is sufficient to initiate morphological changes to the adherent cells. In a different approach, shape-changing scaffolds were FDM-printed with graded, interconnected pores, from a castor oil/polycaprolactone (PCL) triol mixture [39]. The graded porosity mimicked the nonuniform distribution of the pores present in natural tissues and promoted the adhesion, proliferation, and differentiation of human MSC (hMSC). Self-fitting porous scaffolds for bone defects have also been printed with FDM using polylactide (PLA) and hydroxyapatite as materials [40, 41].

3.1.2. Cryo-3DP

Cryo-3DP, another extrusion-based technique, utilizes the liquid to solid phase transition of a hydrogel ink [42]. The extruded material is printed in a liquid coolant, such as liquid nitrogen [43] or an isopropanol bath with solid carbon dioxide (CO_2) [42], where it is cooled below its freezing point (figure 2(b)). This method permits the fabrication of stable, complex structures from hydrogels with low viscosity values. Cryogenic 3D printing has been used for the fabrication of shape-changing scaffolds from β-tricalcium phosphate and poly(lactic acid-*co*-trimethylene carbonate) nanocomposite solutions for the treatment of irregular bone defects [29]. In that study, the scaffolds were printed at −10 °C and were compressed to a very small volume. They then regained their shape upon exposure to near-infrared irradiation. The implantation of the compressed constructs in rat cranial defects resulted in improved formation of new bone. The majority of the reviewed studies used an extrusion-based fabrication method, whether it was for conventional printing or bioprinting. This trend may be justified by the simplicity of the extrusion printing technologies as well as the option they offer to use hydrogels with or without cells directly as inks (e.g. in DIW, cryogenic 3D printing).

3.1.3. DIW

DIW is a printing technique that utilizes liquid or paste-like materials as inks, which exhibit viscoelastic behaviour in heat-free environments [44, 45]. This enables the use of a broader range of ink materials, as compared to FDM, that can be application-specific. However, DIW requires post-processing steps for solidification that can be time-consuming. Materials that have been used in DIW applications include nanocomposite polymeric solutions [46], hydrogels [47], resins embedded in a supporting matrix [48], metal/bioceramic-based inks [49] and ceramic slurries [50]. The inks are placed in a reservoir or cartridge and extruded as continuous filaments using a pneumatic pump or a mechanical piston or screw (figure 2(c)). The printed constructs solidify through either a temperature phase-change or a crosslinking/gelation mechanism. DIW has been implemented for the fabrication of highly stretchable scaffolds with shape memory and self-healing properties, using an ink containing urethane diacrylate and PCL, which can be used as 'patches' for vascular repair [51]. In addition, Wang *et al* [52] used DIW for the fabrication of shape-shifting scaffolds from alginic

Table 1. Classification of the reviewed studies on the applications of 4D printing in TERM, based on the (bio) printing method, the printing resolution, and the material used as ink.

Class	Method	Resolution (μm)	Material	References
3D printing	FDM	160–170	Aromatic shape memory polyurethane functionalized with type I collagen	[38]
		250	Sacrificial 3D printed scaffold: PLA, Filling material: castor oil and PCL triol	[73]
		350	PLA with hydroxyapatite nanopowder	[40, 41]
		350	PNIPAAm/poly(HEMA)	[26]
	Cryo-3DP	400	β-tricalcium phosphate P(DLLA-TMC) with black phosphorus	[29]
		260	AA coated with silver nanoparticles	[74]
		300	PGDA	[75]
	DIW	600	PCL	[51]
		337	AA/PNIPAAm hydrogels	[47]
		400	AA/Pluronic F127 diacrylate	[52]
	SLA/DLP	400–430		[61]
		∼120	Soybean oil epoxidized acrylate	[25]
		various		[62]
		300	PEGDA and BPADMA	[76]
		150	Methacrylated PCL	[77]
		200	Aliphatic Poly(carbonate) Urethanes	[64]
		25	Bisphenol diglycidyl ether and graphene	[78]
	Inkjet	140	Gel-MA/Gel-COOH-MA	[71]
	Hybrid	330	Extrusion: AA-MA	[67]
		200	MEW: PCL	
3D bioprinting	Extrusion- based	260	AA-MA and HAMA	[60]
		603	Phase 1: AA/PDA, Phase 2: AA/Gel-MA	[79]
		184	Gel-MA	[28]
		300	OMA, GelMA, PEGA8	[80]
		300	OMA	[81]
		200	AA and HAT	[27]
	DLP	40	Silk fibroin/glycidyl methacrylate	[65]
		100	GelMA and PEGDM	[82]

acid or alginate (AA)/pluronic F127 diacrylate hydrogels, illustrating their potential application in TERM.

3.1.4. Extrusion-based bioprinting

In extrusion-based bioprinting, the bioink is extruded through one or more nozzles as a continuous filament based on either a pneumatic or mechanical extrusion system, as described for DIW (figure 2(c)). A pneumatic system increases the structural integrity of the printed scaffold [53], while its mechanical counterpart can allow for a more direct control over the bioink flow than the pneumatic system which can suffer from a delay of the compressed gas used. Although this printing method is a subcategory of DIW technologies, the use of inks combined with living cells is a unique feature which has resulted in the term extrusion-based bioprinting to prevail in the TERM field. A wide range of bioinks can be printed using this technology, including hydrogel precursor solutions [54] as well as cell pellets or aggregates [55]. The viscosities of the bioinks used to date range between 30 mPa·s to $\geqslant 6 \times 10^7$ mPa·s [56]. However, the mechanical stress developed between the inner walls of the nozzle and the bioink can become very high and have a negative impact on cell viability [20, 57]. To alleviate this issue, materials with shear thinning behavior (i.e. a decrease in viscosity upon the increase of the applied shear rate) are often preferred for extrusion applications. For such materials, the high shear rate value at the nozzle-tip acts as a printing optimization parameter. As the viscosity decreases under applied shear stress, the bioink flows more smoothly through the nozzle and, upon deposition on the printing platform and in the absence of applied shear stresses, the viscosity increases again resulting in the shape-retention of the deposited filament. Nevertheless, maintaining a high cell viability remains a challenge and requires careful tailoring of certain printing parameters, such as the inner nozzle diameter and geometry, the applied pressure, and the printing speed, depending on the viscosity of the bioink used in this process. A detailed overview on bioink printability and the different parameters that affect it can be found elsewhere [58, 59].

As an example of 4D bioprinting, an extrusion-based system developed by Kirillova *et al* [60] have

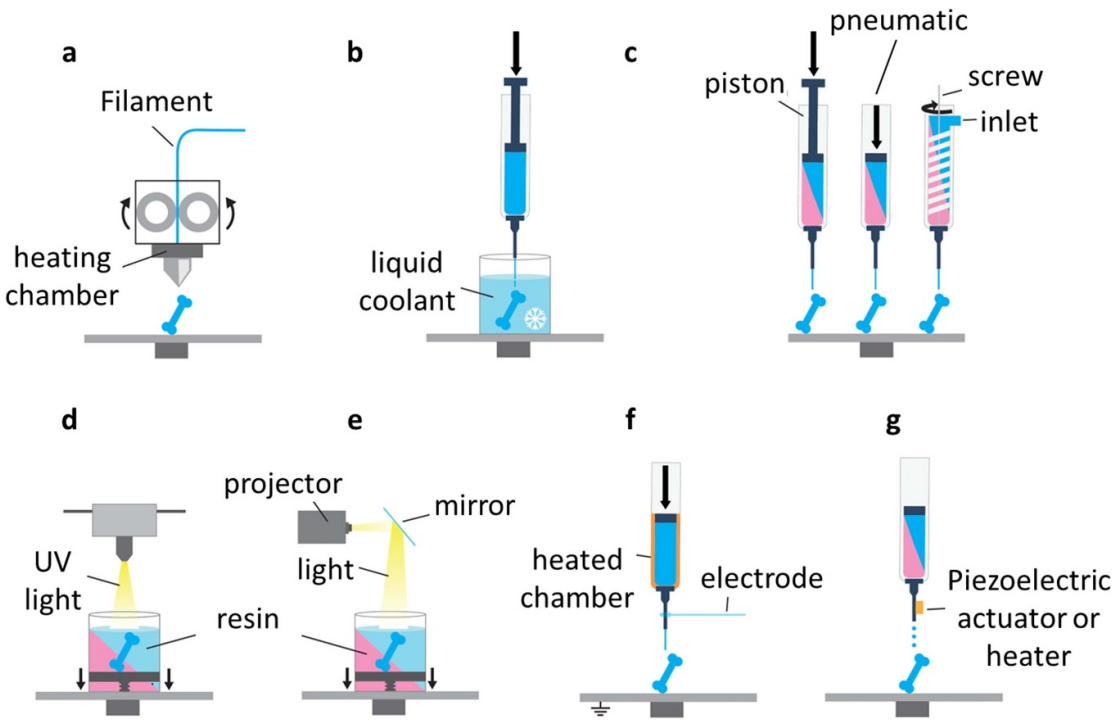

Figure 2. 3D fabrication methods used in 4D (bio)printing and their presence in TERM applications. (a) Fused deposition modeling (FDM), (b) cryogenic 3D printing, (c) direct ink writing (DIW), and extrusion-based bioprinting, (d) stereolithography (SLA), (e) digital light processing (DLP) (bio)printing, (f) melt electrowriting and (g) inkjet printing. Blue: cell-free ink. Pink: bioink.

been used for the fabrication of self-folding tubes composed of two types of cell-laden hydrogels based on AA and hyaluronic acid (HA). When submerged in aqueous media, printed mats with thickness values varying between 2 μm and 16 μm folded (in the order of seconds) into hollow, tubular structures with diameters comparable to the diameters of the smallest blood vessels and could support cell survival for at least 7 days [60]. In a different approach, a gelatin methacryloyl bioink was simultaneously extruded through a nozzle to produce thin hydrogel fibers and was exposed to electrical stimulation before crosslinking, which induced gelatin and cell alignment. The fibers were deposited on a self-folding gelatin film to mimic the formation of myotube bundles [28].

3.2. Light-based

3.2.1. SLA

SLA uses a single-beam ultraviolet (UV) laser to crosslink or polymerize a photopolymer resin in a layer-by-layer manner [37]. The UV laser is directed to the desired coordinates across the *xy* plane, tracing the geometry of each layer and curing the resin in a point-by-point manner (figure 2(d)). Using soybean oil, epoxidized acrylate as resin, Miao *et al* fabricated temperature-activated complex scaffolds using SLA [61] and demonstrated their successful applications as tubular nerve guidance conduits in a later study [25]. Moreover, by combining SLA with photolithography, the authors reported the fabrication of self-foldable scaffolds capable of supporting cardiomyogenic differentiation, thus showing the potential of these 4D constructs for cardiac TERM applications [62].

3.2.2. DLP

DLP is a printing method similar to SLA. The primary difference between the two techniques is the light source: DLP uses light from a projector (UV or white light) instead of a laser (figure 2(e)). Additionally, in DLP, the light source remains stationary, curing a complete layer of resin at a time [63]. Weems *et al* used DLP for the fabrication of shape-memory scaffolds from aliphatic polycarbonate urethanes for the induction of adipose tissue repair [64].

3.2.3. SLA- and DLP-based bioprinting

SLA and DLP have also been modified for bioprinting. The working principles of such systems are similar to the ones described before: a photocrosslinkable bioink is solidified layer-by-layer by a light source. High resolution in combination with rapid fabrication make SLA and DLP attractive bioprinting methods. However, certain drawbacks of these methods, such as the continuous photocrosslinking of already printed layers should be considered, as they can affect the functionality of the structure by introducing a

stiffness gradient, which can then be used as 4D strategy. For instance, a novel 4D bioprinting system based on DLP and a UV-curable, cell-laden silk fibroin bioink was employed by Kim *et al* [65] for the fabrication of trachea-mimetic tissue scaffolds that can swell to a desired curved shape. Patterned sheets with various designs, including flowers, *Dionaea*, clams, and stars were also printed achieving a layer thickness of 40 μm [65].

3.3. MEW

MEW is a 3D printing technique based on melt electrospinning principles that combines some elements of electro-hydrodynamic fiber attraction and melts extrusion [66] (figure 2(f)). MEW allows for the consistent production of fibers in the submicron range with a relatively high surface area and can be used to fabricate 3D patterned scaffolds with increased dimensions along the extrusion axis. MEW has been used for the fabrication of methacrylated AA and PCL bilayers capable of self-folding when immersed in aqueous solutions. The tubes were found to support high myoblast viability and proliferation as well as an increased degree of cell orientation along the direction of the PCL electrowritten fibers post-4D transformation [67].

Although not considered as 3D printing, electrospinning has also been used in 4D approaches to create shape-changing structures. For instance, uniaxially aligned PCL-poly(glycerol sebacate) (PCL-PGS) and randomly aligned methacrylated HA fibers were combined in bilayers and self-folded into tubular structures upon immersion in an aqueous buffer [68]. In a similar approach, a layer of aligned PCL fibers was electrospun on top of a layer of anisotropic methacrylated alginate (AA-MA) fibers. The scroll-like self-folded mats directed the differentiation of myoblasts into aligned myotubes that contracted upon electrical stimulation [69].

3.4. Inkjet-based

Inkjet printing is the most commonly used type of printing for both non-biological and biological applications [20]. In inkjet printing, the ink is loaded in a cartridge connected to a printing head, which ejects the material in drops, following the object profile. There are two kinds of drop-on-demand heads: piezoelectric and thermal (figure 2(g)). In thermal systems, a heating element (e.g. thin-film resistor) is attached to the inner walls of the head. When an electrical pulse is applied, a high current flow through the resistor, causing the ink in contact with it to evaporate and form a bubble. The expansion of this bubble increases the pressure in the ink, leading to the ejection of a droplet from the nozzle. In piezoelectric inkjet printing, a piezoelectric actuator is attached to the printing head and, upon the application of a voltage pulse, induces a volumetric change to the ink reservoir. This change leads to a pressure increase which subsequently results in droplet ejection [70]. Thermal inkjet printers have a higher printing speed and lower fabrication cost as compared with their piezoelectric counterparts. However, piezoelectric systems possess a high control on the size and directionality of the generated droplets without increasing the ink temperature [20]. The selection of the inkjet system depends on the desired properties of the scaffold and the shape transformation strategy.

An inkjet platform for 4D printing was developed by Cui *et al* to fabricate bilayers synthesized from gelatin-based materials [71]. Immersion in aqueous media resulted in the self-rolling of the scaffolds into microtubes that could successfully mimic microvessels and support the encapsulation and proliferation of endothelial cells. Droplet-based printing has also been used for producing synthetic cells that could self-assemble into tissue-like structures capable of folding in a controlled manner after light stimulation, thus showing potential for 4D bioprinting [72].

4. Stimuli used for shape transformation

Shape transformation in 4D (bio)printed scaffolds is triggered by the application of one or more stimuli, post-fabrication. In this section, we review the different stimuli that have been used for TERM applications.

4.1. Hydration

Hydration was identified as one of the most popular stimuli investigated in current 4D (bio)printing approaches for shape-shifting. Many native tissues are responsive to changes in the humidity of their environment. The responses can range in complexity from the curling of drying leaf to self-burial of the *Erodium cicutarium* seeds [83]. Another common example of tissue response to environmental humidity is that of the pine cones. Pine cones, which are natural hygromorphs, are closed in the presence of a humid environment and 'open' when they dry [84]. Such hygroscopic behaviors inspired the study and development of humidity-responsive materials as 4D printing inks for the fabrication of shape-changing structures using hydrogels.

Hydrogels are hydrophilic, three-dimensional networks of physically or chemically crosslinked polymers that can absorb and retain a large fraction of water while remaining insoluble. They are composed of an aqueous matrix and, in addition to humidity, may respond to other external stimuli, such as temperature [85] or light [86], as well as demonstrate shape-memory behavior [52]. Hydrogels that have been used for the preparation of inks for 4D printing of shape-shifting structures include HA [27, 60], AA [27, 60, 67, 80], gelatin [28, 71, 80], and silk fibroin [65]. Stimulation of shape transformation with humidity is achieved by submerging the

printed hydrogel scaffolds in a swelling medium (e.g. water, PBS, or cell culture medium). Humidity is a stimulus suitable for both cell-free and cell-laden constructs. For the latter, the swelling medium is a cell culture medium, and the swelling temperature is 37 °C. Apsite *et al* fabricated bilayer scaffolds consisting of a layer of aligned PCL fibers and a layer of anisotropic AA-MA fibers [69]. When submerged in water, the bilayers rolled and formed tubular scroll-like structures, due to the swelling of the AA layer. The diameters of these microtubes and the folding side of the scaffolds could be tuned by changing the orientation of the PCL fibers as well as the thickness of the AA layer. In a different 4D bioprinting approach, cell-laden bars consisting of a layer of oxidized AA-MA and a layer of GelMA exhibited controlled bending upon immersion in growth medium (figure 3(a)) [80]. Incorporation of hMSCs in the hydrogel formulations as well as the use of osteogenic medium resulted in bone-like tissue formation. Multiple synthetic polymers can be modified to acquire shape-shifting properties induced by humidity. For instance, Naficy *et al* investigated the reversibility of shape-change in scaffolds consisting of a bottom part made from a poly(HEMA)-based hydrogel and a top part made from a PNIPAAm-based hydrogel [26]. In a recent study, a low-swelling bioink made of AA and HA and a high-swelling HA ink were used to fabricate bilayers with self-bending behaviors [27]. The final aim was to 4D bioprint a scaffold that mimicked the curved multilayered cellular structure and organization of the native articular cartilage which is a curved structure that needs to have a very smooth surface and is, thus, extremely difficult to fabricate using a layer-by-layer, extrusion 3D bioprinting system.

4.2. Temperature

Temperature is a widely investigated stimulus for shape-shifting in smart materials [31]. This trend was also apparent in 4D printing for TERM applications (figure 1(e) and (f)). The ease of application and the ability to tune the triggering temperature by changing the material composition are the main advantages that have made temperature-responsive materials attractive for TERM applications, with many of the reviewed studies selecting temperature as the trigger of the shape-transformation phase, either as a single stimulus [38, 40, 41, 47, 51, 61, 73, 76, 77, 87, 88] or in combination with other types of stimuli [25, 29, 62, 89].

The materials primarily used for the fabrication of temperature-responsive scaffolds in TE are shape memory polymers (SMPs) (figure 3(b)). For a thorough overview of the applications of thermoresponsive polymers in the biomedical field, the reader is referred to [90]. Different 4D applications have been described for such SMPs. For instance, scaffolds made of shape-memory polyurethane were 3D printed, compressed to a temporary shape at 65 °C, and cooled at 4 °C to fix the temporary shape. The samples were heated to 30 °C, below the glass transition temperature of the polymer (T_g = 32 °C) before cell seeding, and subsequently recovered their initial shape upon heating above their T_g [38]. This allowed the researchers to create a biomimetic environment in which to study the effects of dynamic mechanical properties, typical in an active body, on tissue regeneration. Such approaches have the potential to direct cell activity through mechanotransductive cues. A similar approach was adopted by Miao *et al* [73] using 3D printed shape-memory scaffolds made of PCL. The potential for implanting such scaffolds by using minimally invasive procedures for treating bone defects was demonstrated by uniaxially compressing the samples by almost 30% and allowing them to fully recover to their initial shape when the temperature increased up to 37 °C.

4.3. Light

Apart from hydration and temperature, light has also been used to trigger shape changes in 4D printing. The advantages of light as a stimulus include its local nature that allows for accurate focusing as well as rapid switching. The potential of using light as a stimulus for shape transformation in TERM was demonstrated by Luo *et al* who fabricated 3D printed, biphasic scaffolds, consisting of an AA/polydopamine (PDA) phase and a cell-laden AA/gelatin methacryloyl phase [79]. The incorporation of PDA, which has a near infrared radiation (NIR)-responsive behavior and has been used in various biomedical applications to trigger drug release and hyperthermia [91], resulted in NIR-triggered dehydration of the rectangular scaffolds, transforming them to saddle-like structures. The dehydrated scaffolds could maintain their shape in culture media and the incorporated cells showed high viability for up to 14 days [79]. Myocardium-mimetic smart scaffolds consisting of an SMP and graphene (figure 3(c)) have also been fabricated using NIR laser stimulation for triggering the shape-shifting effect. The smart scaffolds were found to support uniform cell alignment as well as tissue maturation [78].

4.4. Multiple stimuli

A combination of two or more of the stimuli presented above can be used to trigger shape transformation multiple times. Miao *et al* developed scaffolds from soybean oil, epoxidized acrylate which could self-transform upon immersion in ethanol (figure 3(d)) and also possessed a shape-memory behavior that was triggered by temperature increase [25, 62]. A photothermal-responsive ink was developed for 4D printing scaffolds to treat critical-size bone defects by incorporating black phosphorus nanosheets in β-tricalcium phosphate/shape memory poly(lactic

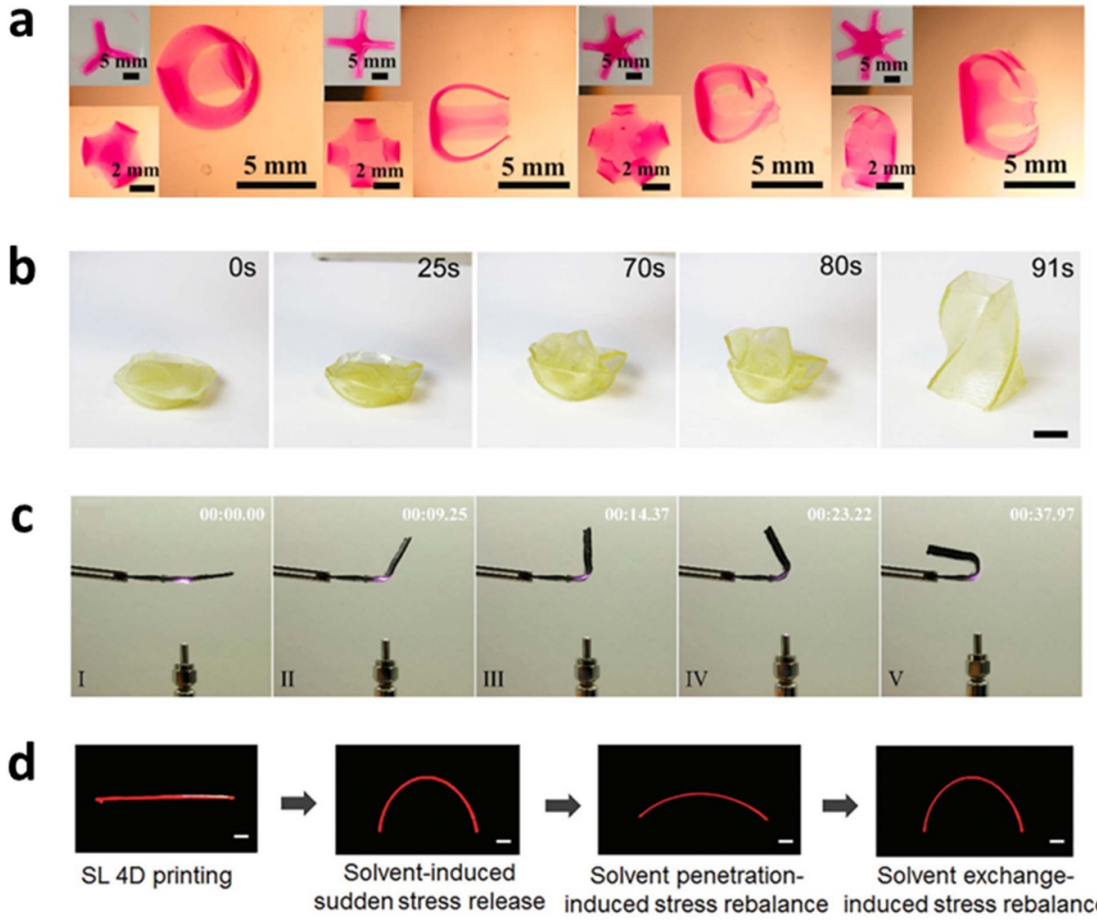

Figure 3. Application of various stimuli in 4D printing. (a) Biofabricated grippers with multiple arms before (top left inset) and after deformation. Hydrogel deformation was performed in a growth medium at 37 °C. Reprinted from [80], Copyright (2021), with permission from © 2021 The Authors. Publishing services by Elsevier B.V. on behalf of KeAi Communications Co. Ltd. (b) A compressed structure recovers to its original shape of a standing hollow vase after being heated. Scale bar: 6 mm. Reprinted with permission from [51]. Copyright (2018) American Chemical Society. (c) The images of a U-shaped structure recovered by NIR laser stimulation. Reprinted with permission from [78]. Copyright (2021) American Chemical Society. (d) 4D printing using stress-induced shape transformation based on multiple stimuli: hydration (water) and dehydration (ethanol). Scale bar: 2 mm. [25] John Wiley & Sons. © 2018 WILEY-VCH Verlag GmbH & Co. KGaA, Weinheim.

acid-co-trimethylene carbonate) (TCP/P(DLLA-TMC)). NIR-induced hyperthermia of the fabricated structures triggered their shape shifting from a temporary compressed configuration to a permanent one to facilitate minimally invasive delivery to the damaged tissue [29].

5. Shape-shifting mechanisms

To transform the shape of 3D printed scaffolds, materials are used that undergo large changes, either physical or chemical, as a consequence of exposure to various stimuli. Based on the application, the engineered scaffolds could be implanted after the 4D shape transformation has occurred, for instance in scaffolds intended to guide maturation *in vitro* and consider implantation at a later stage [28, 60, 65]. However, most of the studies reviewed here considered the case of triggering the shape-change after the scaffold was implanted at the site of interest [51, 61, 73, 77]. Two shape transformation mechanisms have been mostly explored for 4D printed scaffolds intended for TERM applications, namely, shape-memory and differential swelling.

5.1. Shape-memory effect

Shape-memory materials can memorize permanent shapes, be brought to a temporary shape, and recover to their original conformation upon exposure to a stimulus, such as temperature [92], moisture [93], light [94], or a magnetic field [95]. A full cycle of a shape-memory material includes two phases, namely the programming and the recovery steps. During the programming step, the material is deformed to a temporary shape, while during the recovery step it self-transforms back to its original, permanent shape, following stimulus application. Here, we will focus on thermoresponsive SMPs (figure 4(a)), as they have attracted significant interest for shape-memory-based 4D printing applications (table 2).

Polymers exist in a glassy state at low temperatures and a rubbery state at elevated temperatures.

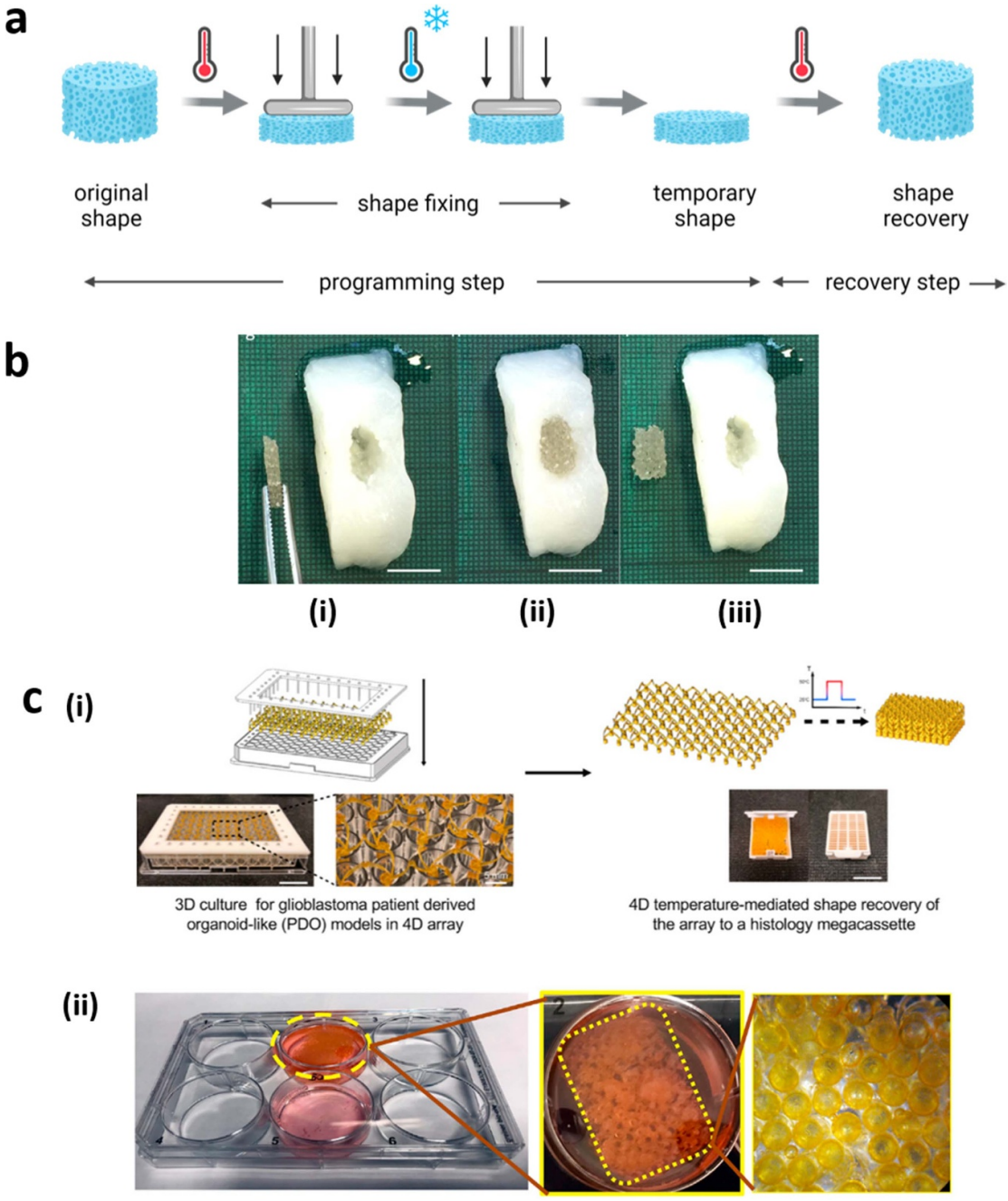

Figure 4. Shape memory-based 4D printing. (a) A schematic illustration of the programming and recovery steps of a thermoresponsive shape-memory scaffold. Created with BioRender. (b) *In vitro* void filling of a DLP printed polyurethane-based implant, demonstrating the shape-memory behavior of the porous scaffold. (i) The temporary shape after programming, (ii) shape recovery in the void, without visible deformation of the void-bearing structure and (iii) removal of the scaffold for further inspection of the recovery process. Scale bars: 1 cm. Reproduced from [64]. CC BY 4.0. (c) (i) Stretched 4D culture array to a 96-well plate configuration (temporary shape) and its recovery to a histology megacassette configuration. (ii) The megacassette containing patient-derived glioblastoma organoids cultured in a 6-well plate. Reprinted from [76], Copyright (2020), with permission from Elsevier.

In the rubbery state, polymers can withstand large deformations. If the temperature is lowered from the rubbery state, while the deformation of the polymer is kept constant, a temporary shape can be fixed in the glassy state. As the glassy modulus is at least two orders of magnitude higher than the rubbery modulus, the elastic stress stored in the polymer is not large enough to drive shape recovery after the load is removed in the glassy state. Upon reheating to the rubbery state, ordinary polymers are incapable of completely restoring the residual inelastic deformation. On the contrary, thermoresponsive SMPs can recover almost the entire residual deformation [96]. The driving force for the shape recovery is a change in the mobility of the polymer chains and a transition from an ordered, temporary configuration to a thermodynamically favored configuration of higher entropy [40]. The threshold

Table 2. The shape-memory parameters used in the reviewed 4D printing applications.

Material	Programming step		Recovery step	References
	$T_{f,\,\text{high}}$ (°C)	$T_{f,\,\text{low}}$ (°C)	T_r (°C)	
TCP/P(DLLA-TMC)	45	37	45	[29]
PLA and hydroxyapatite	80	RT	80	[40]
PLA and hydroxyapatite	64	RT	64	[41]
Semi-IPN elastomer composites	70	0	70	[51]
Soybean oil epoxidized acrylate	37	−18	20	[61]
Polycarbonate-based polyurethanes	37	25	37	[64]
Aromatic polyurethane (MM 3520)	65	15	32	[38]
PCL triol and castor oil	37	−18 or 0	37	[73]
PEGDA and BPADMA	50	25	50	[76]
Graphene-doped bisphenol A diglycidyl ether	80	0	80	[78]
PGDA	37	20	37	[75]

$T_{f,\,\text{high}}$: the heating temperature for the beginning of the programming step. $T_{f,\,\text{low}}$: the cooling temperature for fixing the temporary shape. T_r: the shape-recovery temperature. RT: Room temperature.

temperature to activate the recovery is called the transition temperature (T_{trans}) and can be tailored by altering the composition, concentration, or cross-linking degree of the polymers [97]. Shape-memory materials for 4D printing include polyurethane based [38, 64], PCL-based [51, 73], and PLA-based inks [40, 41] as well as soybean oil, epoxidized acrylate (table 2) [61].

To assess the efficiency of shape recovery in SMPs, two parameters are usually determined: the shape recovery rate (R_r) and the shape fixity rate (R_f). R_r quantifies the extent of shape recovery whereas R_f measures the ability of the SMP to maintain its deformed shape in the glassy state after the external load is removed [98]. R_r and R_f are determined by the following formulas:

$$Rr\,(\%) = \frac{\varepsilon_m - \varepsilon_p\,(N)}{\varepsilon_m - \varepsilon_p\,(N-1)} \times 100 \qquad (1)$$

$$Rf\,(\%) = \frac{\varepsilon_u\,(N)}{\varepsilon_m} \times 100, \qquad (2)$$

where ε_m is the maximum strain of the SMP that is kept constant during the cooling phase of the programming step, ε_p is the residual strain that is left at the end of the recovery step, ε_u is the recovered strain after removing the load from the structure during the programming step, and N is the loading cycle. In applications where the fabricated objects are deformed by bending or rolling during the programming step, R_r and R_f can be determined using the deformation angle [52, 61, 73] or cylinder diameter [88], respectively.

In 4D printing, the permanent shape of SMP-based inks is defined by the 3D printed structure. This structure is subsequently deformed and cooled for fixing the temporary shape. Upon increasing the temperature to reach the rubbery state of the applied SMPs, the deformed structure recovers its original, 3D printed shape. In biomedical applications and especially for TE and RM, the threshold temperatures for the shape-memory cycle must be tailored wisely to be compatible with the tolerance of the incorporated functional molecules, cells, and/or surrounding tissues. So far, a wide temperature range has been used with fixing temperatures varying between −18 °C [25, 61, 62, 73] and 25 °C [76] and recovery temperatures ranging from 37 °C [38, 73, 76] to 70 °C [40].

The main focus of 4D printed, shape-memory scaffolds demonstrated to date for TERM applications appears to be the development of constructs that can be implanted via minimally invasive strategies at a defect site. More precisely, by reducing the size of the scaffold during shape fixation, its delivery and fitting to the site of interest can be optimized. Decreasing the diameter of cylindrical structures in the programming step allows for the *in vitro* introduction of endoluminal [77] and vascular [51, 75] stents that could securely anchor to the native tissue (trachea and blood vessels, respectively), upon recovering to their original shape. Furthermore, compressed scaffolds capable of recovering to a larger geometry have been used for filling bone cavities (figure 4(b)) [29, 40, 41, 73]. In addition, more advanced 4D printing approaches using shape-memory materials have been proposed. For instance, a multiwell array insert printed by projection micro-SLA was recently reported for culturing patient-derived glioblastoma organoids [76]. The array could be stretched to a 96-well plate conformation (temporary shape) and, upon heating to $>T_{\text{trans}}$, recover to its original shape which was programmed to precisely fit in a histology cassette, thus facilitating post-processing tissue analysis (figure 4(c)).

In addition to thermo-responsive SMPs, there are other shape-memory mechanisms, such as ionic-responsive SMPs, that could be of interest in 4D printing applications. For instance, Lu *et al* used a combination of Ca^{2+} or Fe^{3+} ions and high temperature solvents to trigger reversible molecular switches to coordinate metal-ligand and host-guest interactions [99]. Despite the novel aspects of such mechanisms,

the concentration of ions and the high temperature used needs to be revised to ensure cell viability and its applicability in TERM applications.

5.2. Differential swelling

Differential swelling is another mechanism that has been widely employed in 4D printing to fabricate shape-shifting scaffolds, using hydrogel-based inks for TERM applications. Differential swelling has been used for producing mainly tubular or curved structures [28, 60, 65, 71, 74]. One of the approaches using this mechanism is based on the use of a bilayer scaffold containing two materials with distinct swelling profiles [100]. The presence of a hydrophilic layer and a hydrophobic or less hydrophilic layer enables the controlled bending of the bilayer in its thickness direction upon the immersion of the specimen into aqueous solutions (figure 5(a)). Díaz-Payno, Kalogeropoulou *et al* 4D bioprinted a flat bilayered scaffold that was able to curve into a cartilage-mimicking structure using a high swelling HA-tyramine (HAT) and a low swelling HA-tyramine containing AA bioink (AHAT) (figure 5(b)) [27]. A second approach is the control of the photocrosslinking degree throughout the thickness of a scaffold. This can establish a swelling gradient within a single-material to achieve a bending effect [60, 80]. For instance, Kirillova *et al* presented a 4D bioprinting approach for the fabrication of cell-laden hydrogel scaffolds from AA or HA crosslinked from the top capable of self-rolling into hollow tubes when immersed in aqueous media [60]. The tubes retained their shape without showing any signs of degradation even 6 months after their fabrication (figure 5(c)). A third approach for enhancing the swelling-induced shape-shifting is the patterning of one of the two layers (figure 5(d)) [28, 65]. In a different study, the differential swelling of a hydrogel bilayers was used as a hinge-like mechanism for the fabrication of self-assembling cubes (figure 5(e)) [26].

To quantify the degree of shape-change as well as the time needed to reach a stable state, certain material properties and parameters can be determined. A commonly used indicator of the amount of liquid a hydrogel can absorb is the (mass) swelling ratio (Q_m) which is defined as:

$$Qm = \frac{m_s}{m_d}, \tag{3}$$

where m_s is the mass of the swollen hydrogel polymer and m_d is the mass of the dry hydrogel. The swelling ratio and, by extension, the degree of shape-change of 4D printed scaffolds can be controlled by tailoring several parameters. In terms of ink-related parameters, the composition of the hydrogel [80] as well as the crosslinking degree [28, 60, 67] have been used to control how far the scaffolds self-bend. For instance, photocrosslinking Gel-MA films for 10, 30, and 60 min resulted in structures with swelling ratios of ∼150%, ∼300%, and ∼350%, respectively [28]. The scaffold design has also been reported to affect the final shape. By tuning the thickness ratio of the two layers [67, 71], the thickness of the whole scaffold [28, 60, 71, 80] as well as the pattern design or orientation [65, 67], the shape-shifting can be further controlled. Finally, a swelling-dependent system can be affected by the composition of the swelling medium [60, 65, 67, 80] as well as the concentration of certain ions in the medium [68, 69], which can modulate the degree of shape-change. More specifically, the reported swelling ratios of HA-based mats varied between 2000%, 3000%, and 4000% after 24 h in water, PBS, and, culture medium, respectively. An overview of the characteristic parameters of the reviewed studies is presented in table 3.

In several studies, efforts have been made to predict the swelling-induced bending and curvature values [12, 24, 71]. Those predictive models are inspired by the Timoshenko equation, which was originally developed to predict the bending of bi-metal beams subjected to uniform heating [101]. In differential swelling, however, the driving force of bending is the difference between the swelling ratios of both layers, instead of their coefficients of thermal expansion. Therefore, certain assumptions and modifications of the classic model have been proposed. Firstly, as the bending is not triggered by temperature variations, the temperature difference can be ignored to a certain extent. Secondly, the 3D printed layers of the structure are considered uniform and isotropic, but this is not always the case. Thus, the introduction of correction coefficients to compensate structural and material heterogenicity as well as the addition of the swelling ratios to the original equation have also been suggested [71].

5.3. Other mechanisms

Apart from thermoresponsive shape-memory effect and differential swelling, other shape-changing mechanisms have also been used for 4D printing. The coil-globule transition of PNIPAAm hydrogels is a mechanism underlying large, reversible volume changes at a critical temperature (≈32 °C − 35 °C) and results in a dramatic decrease in the water content when the temperature is increased above that critical value. By combining PNIPAAm with AA, interpenetrating polymer network hydrogels compatible with extrusion (bio) printing were prepared and, subsequently, used for the fabrication of thermally actuating scaffolds that swell and shrink reversibly [47]. In a different approach, electrospun PCL-PNIPAAm-PCL trilayers capable of folding into tubular structures were fabricated [89]. The thermo-sensitivity of PNIPAAm defined the folding degree and side while the fiber orientation of the PCL layers defined the folding direction [89]. Furthermore, the drying of AA has been used as a mechanism for inducing shape-shifting of 3D printed scaffolds [79].

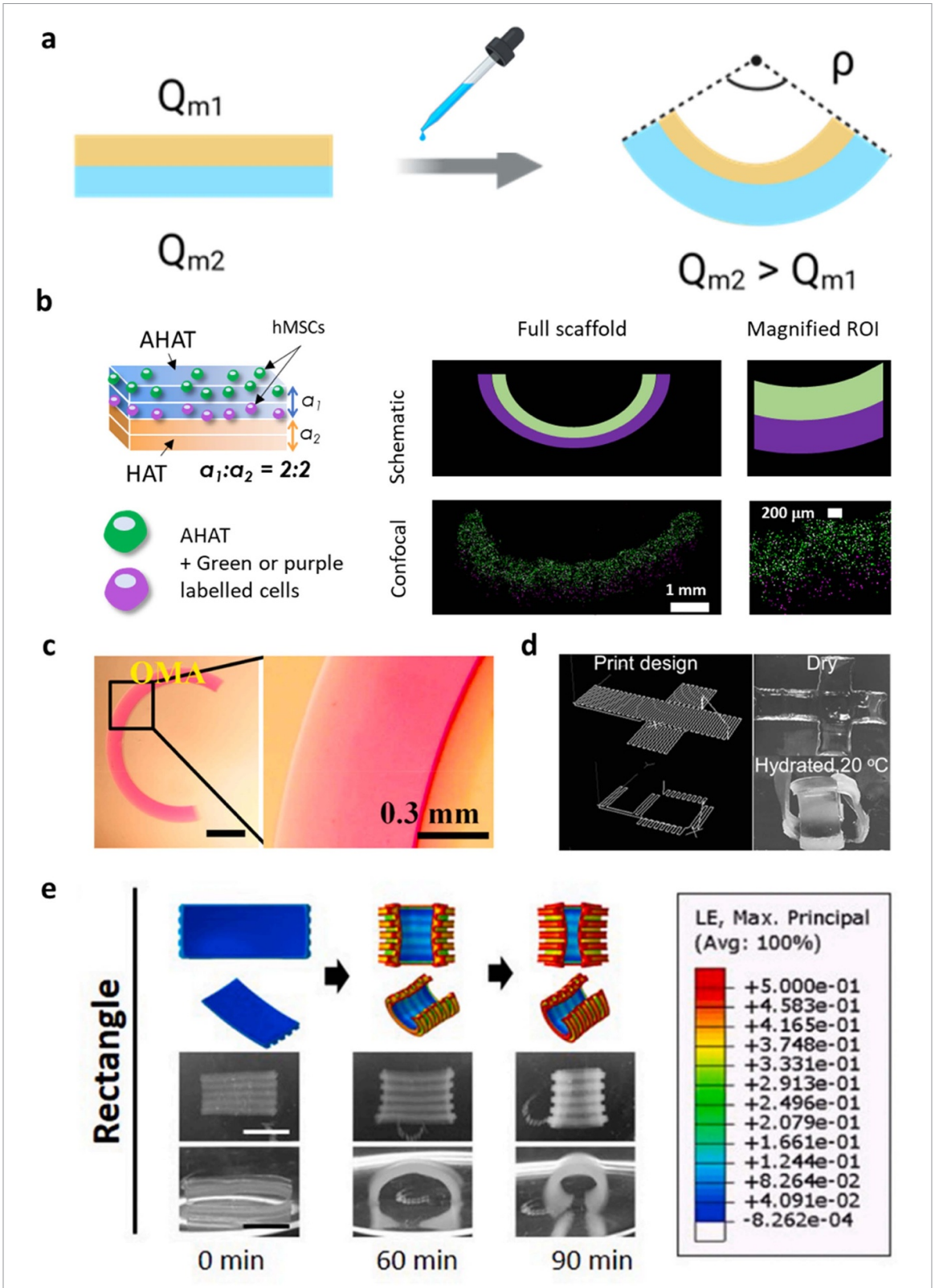

Figure 5. Differential swelling-based 4D printing. (a) An illustration of the bending of a bilayer scaffold due to the distinct swelling ratios (Q_m) of both layers, upon stimulation with an aqueous solvent. Created with BioRender. (b) A proof-of-concept of the fabrication of a curved multilayered cellular construct made of AA with HA-tyramine (AHAT) and HA-tyramine alone (HAT) where bioprinted human mesenchymal stromal cells (hMSCs) remained in their corresponding layers after the 4D transformation. Reproduced from [27]. CC BY 4.0. © 2022 The Authors. Advanced Healthcare Materials published by Wiley-VCH GmbH. (c) (left) Bending of a scaffold made from oxidized and AA-MA (OMA) with a continuous crosslinking gradient across its thickness. Scale bar: 2 mm. (right) A magnified image clearly showing the gradient. Reprinted from [80], Copyright (2021), with permission from © 2021 The Authors. Publishing services by Elsevier B.V. on behalf of KeAi Communications Co. Ltd. (d) The printing pattern of a cubic box and its hinges (actuating parts) and some images of the box in its as-printed (top) and swollen (bottom) states. The base of the box was printed using a NIPAM-based ink while the hinges were printed from a poly(HEMA) based ink. [26] John Wiley & Sons. © 2016 WILEY-VCH Verlag GmbH & Co. KGaA, Weinheim. (e) Finite element analysis (FEA) simulation (top) and experimental results (bottom) of a bi-layered scaffold made from silk fibroin with a patterned layer. Reprinted from [65], Copyright (2020), with permission from Elsevier.

Table 3. The differential swelling parameters used in 4D printing applications showing different layer composition, pattern design (or orientation), swelling strategy and bending control.

Layer 1	Layer 2	Pattern	Swelling strategy	Bending control	References
AA-MA or HA-MA	—	No	Crosslinking gradient	Layer thickness, swelling medium, crosslinking time, printing speed	[60]
Gel-MA	Gel-MA	Yes	Patterning	Crosslinking time, bilayer thickness pattern	[28]
Sil-MA	Sil-MA	Yes	Crosslinking gradient	Swelling medium, pattern culture time	[65]
AA-MA	PCL	Yes	Distinct swelling ratios	Crosslinking time, pattern thickness ratio, Ca^{2+} concentration, swelling medium	[67]
Gel-COOH-MA	Gel-MA	No	Distinct swelling ratios	Temperature, thickness ratio, bilayer thickness	[71]
HAT	AHAT	Yes	Distinct swelling ratios	Crosslinking time, pattern thickness, scaffold pattern, swelling medium	[27]
OMA, Gel-MA or PEGA8	—	No	Crosslinking gradient	Crosslinking time, polymer concentration thickness, swelling medium	[80]
poly(HEMA)based PEO-PU	pNIPAM-based PEO-PU	No	Distinct swelling ratios	—	[26]
OMA	—	No	Crosslinking gradient	Crosslinking time, swelling medium, scaffold dimensions	[81]
GelMA and PEGDM	—	Yes	Crosslinking gradient	Crosslinking time, swelling medium, scaffold pattern	[82]

The combination of more than one shape-changing mechanisms in the same scaffold has also been reported. For instance, laser energy attenuation during the SLA fabrication process has been identified as the source of a crosslinking gradient that resulted in the accumulation of internal stresses in soybean oil-based scaffolds [25, 62]. Immersion in ethanol resulted in stress release and scaffold deformation. A subsequent immersion of the structure in ethanol and water triggered the scaffold to recover and then re-deform, respectively. In addition, the printed scaffolds exhibited shape-memory and could, thus, recover their initial shape after deformation and heating above their T_{trans}.

6. Cell incorporation strategies

Though still in its infancy, 4D printing has been used for the fabrication of scaffolds targeting various tissue types ranging from bone [25, 29, 38, 40, 41, 73], vascular [51, 71], cardiac [62, 79], muscular [28, 38], cartilage [27, 81], and tracheal tissue [65] to synthetic tissues [51] and organoids, such as glioblastoma-derived organoids [76]. Based on the sequence followed from the printing process, the shape shifting, and the encapsulation of cells in the scaffold, three cell-seeding strategies could be identified (figure 6, table 4).

6.1. Strategy 1: Cell incorporation post-fabrication

This strategy includes the fabrication of scaffolds with a conventional 3D printing technique and their subsequent stimuli-induced shape-shifting. Most of the printing methods following this strategy are well characterized methods but most often not cell friendly. As cell encapsulation is not considered in this process, these scaffolds can be used as drug carriers, biomolecules [52, 88], biomedical devices [51, 75, 77], or as off-the-shelf tissue-conductive scaffolds that can be colonized by infiltrating cells post-4D fabrication [25, 41, 61, 64, 73]. This approach allows for greater versatility in the printing method and scaffold design. Additionally, a wide spectrum of different materials can be used, from shape-memory alloys [102] to elastomers [103]. These materials can be processed at elevated temperatures or be crosslinked with potentially cytotoxic radiation wavelengths (UV 365–405 nm) [104] into scaffolds of complex geometries. Unlike the other cell-incorporation approaches, in Strategy 1, the selected stimulus for the 4D transformation may divert from the strictly cell-friendly triggers, without any adverse effects on the biocompatibility of the final scaffold. The mechanical properties of the resulting constructs can also vary greatly, while not being limited to the materials suitable for cell-encapsulation, such as hydrogels. For instance, Wang *et al* fabricated photothermal-responsive shape memory scaffolds for precise fitting in irregular bone

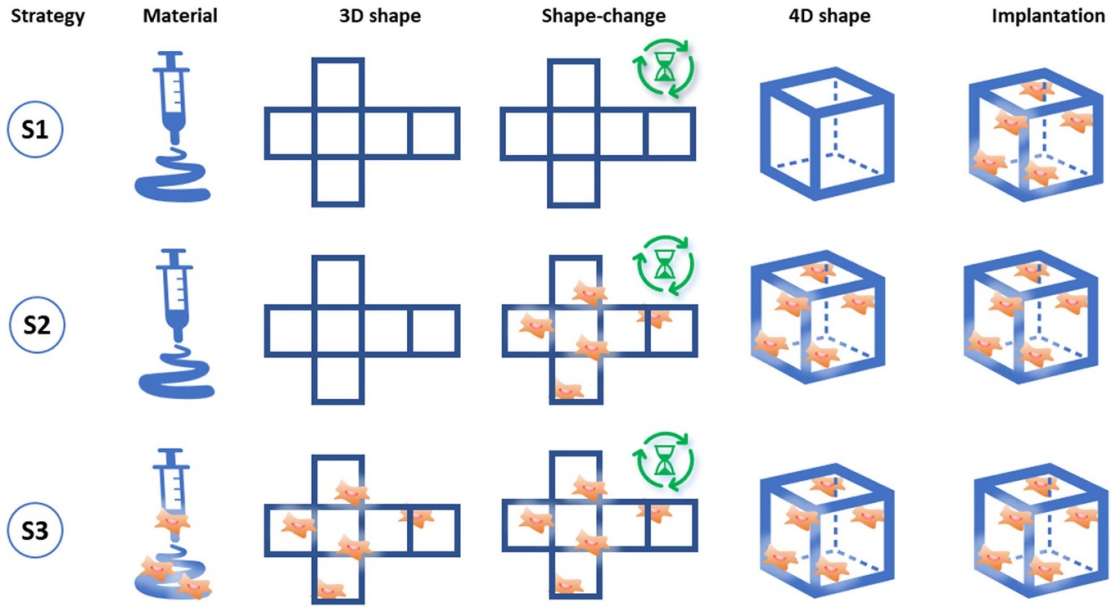

Figure 6. A schematic illustration of the three cell-seeding strategies in 4D printing. From top to bottom: In strategy 1 (S1), no cells are involved in the fabrication process, but after the shape-change has taken place (either added for *in vitro* test or migrated from host upon implantation). In strategy 2 (S2), a cell-free scaffold is printed and is seeded with cells before the stimulation. In strategy 3 (S3), the cells are involved from the beginning of the fabrication process. The scaffold is, thus, bioprinted, using a cell-laden material, and is then exposed to stimulation to change its shape.

defects capable of releasing peptides for enhancing osteogenesis [29, 31]. Nonetheless, it is worth noting that this strategy could require prolonged cell migration times, as the cells are not incorporated in the construct itself, potentially leading to non-uniform tissue growth. To address this challenge, a careful selection of tissue-instructive materials [105], either as the printing material, or as a subsequent coating, may compensate for any fabrication-related issues.

6.2. Strategy 2: Cell seeding post-printing but pre-4D stimulus

In this strategy, the cell seeding follows the scaffold fabrication but precedes the application of the stimuli. Therefore, the structure undergoes shape-shifting after cells have adhered to its surface. This strategy allows for decoupling of the printing process of the two-dimensional unfolded patterns from the incorporation of the cells before the scaffold can transform to a more complex 3D structure [38, 64, 67, 89]. This is particularly useful if the printing technology or crosslinking mechanism utilized is not cell-friendly or leads to a significant decrease in cell viability. For instance, Senatov and colleagues investigated the self-fitting efficiency of shape-memory 3D printed scaffolds that were fabricated using extrusion printing at 180 °C–220 °C. Upon cooling, the scaffolds were used for *in vitro* studies with hMSCs, and demonstrated good biocompatibility and adhesion capacity [41].

Similar to Strategy 1, a broader palette of materials and printing methods can be considered in Strategy 2 as compared to the use of bioinks (Strategy 3). Additionally, a finer degree of control over the initial cell distribution could be achieved with this approach, as different cell types at various densities can be precisely seeded on specific sites of the 3D printed scaffolds. By decoupling the cell seeding and shape-shifting processes, uniform tissue formation is promoted. Following this strategy, Wang *et al* have fabricated patterned cardiac patches that were used for the triculture of hMSCs, hECs, and hIPSC-CMs, using different cell seeding densities for each cell population [78]. In the same study, a comparison of the cell seeding efficiency before and after the application of the 4D stimulus revealed that pre-curved patches were unable to form uniform cardiac tissue, since the cells settled and aggregated at the bottom of the scaffolds due to gravity effects.

Regarding the selection of the proper 4D approach in Strategy 2, it becomes clear that the selected stimulus will be limited by their degree of biocompatibility. In other words, since the shape-shifting occurs after cell seeding, only cell-friendly stimuli can be used to ensure high viability. Moreover, if the selected stimulus is either physiological temperature or/and humidity, the cell seeding step could inadvertently trigger the shape-shifting of the scaffold. This limitation could be potentially addressed through sacrificial materials that delay the programmed shape transformation until the desired moment. For example, Cui *et al* fabricated gelatin-based bilayers, which were kept flat using a sacrificial AA/gelatin layer. After the adhesion, spreading, and proliferation of HUVEC cells, the sacrificial layer was dissolved, allowing the bilayered mat to fold into a tube, due to the difference in the swelling ratios of

Table 4. The cell-seeding strategies and their parameters.

Cell seeding strategy	Target tissue	Cell type	4D mechanism	Material	References
S1	—	—	Shape-memory	Soybean oil epoxidized acrylate	[61]
	Adipose	—	Shape-memory	Polycarbonate-based polyurethanes	[64]
	Bone	—	Shape-memory	PCL triol and castor oil	[73]
		—	Shape-memory	PLA and hydroxyapatite	[40]
		—	Shape-memory	TCP/P(DLLA-TMC)	[29]
	Synthetic	—	Osmolarity	Lipid-coated aqueous droplets in oil	[72]
	Vascular	—	Shape-memory	Semi-IPN elastomer composites	[51]
		—	Shape-memory	PGDA	[75]
S2	Bone		Shape-memory	PLA and hydroxyapatite	[41]
	Bone, Muscle	Mouse MSC	Shape-memory	Aromatic polyurethane	[38]
	Cardiac	hMSCs, hECs, hiPSC-CMs	Shape-memory	Bisphenol diglycidyl ether and graphene	[78]
		hMSC	Differential swelling	Soybean oil epoxidized acrylate	[108]
	Drug delivery	Mouse fibroblasts	Shape-memory	AA/Pluronic F127 diacrylate	[52]
	Glioblastoma		Shape-memory	PEGDA and BPADMA	[76]
	Muscle	Mouse muscle cells (C2C12)	Differential swelling	AA-MA/PCL	[67]
	Neural	hMSC	Stress-induced	Soybean oil epoxidized acrylate	[25]
	Vascular	Glioblastoma-derived cells	Differential swelling	GelMA-COOH/GelMA	[71]
S3	Bone	hMSC	Differential swelling	OMA, Gel-MA or PEGA	[80]
	Cardiac	Human embryonic kidney cells	NIR-induced dehydration	Alg-PDA/Alg-GelMA	[79]
	Cartilage	NIH3T3, HeLa, hMSC	Differential swelling	OMA	[81]
		hMSC	Differential swelling	Alg-HAT/HAT	[27]
	Muscle	Mouse myoblasts	Differential swelling	GelMA/GelMA	[28]
	Trachea	hCC, rabbit CC and turbinate MSC	Differential swelling	Sil-MA/Sil-MA	[65]
	Vascular	Mouse stromal cells	Differential swelling	AA-MA or HAMA	[60]
		Mouse fibroblasts	Differential swelling	GelMA and PEGDM	[82]

both layers [71]. While the limitations of Strategy 2 may be mitigated through meticulous selection of materials, stimuli, and seeding techniques, it is worth acknowledging that the complexity of this approach may inevitably extend the fabrication timeline.

6.3. Strategy 3: Cell encapsulation pre-printing

The third strategy refers to the 4D bioprinting processes when the cells are incorporated in the ink prior to the printing and shape-transformation processes [27, 28, 60, 65, 79, 80]. The advantage of this strategy is the ability to place cells in the desired location during fabrication, while the disadvantage is that the process relies on cell friendly bioinks, which still need further development in terms of printing resolution and fidelity.

In this single-step approach, cells are integrated directly into the structural matrix of the scaffold during the fabrication process, thus reducing the fabrication time and complexity. A good homogeneity of the

printed scaffolds can also be achieved, because cells are incorporated inside the ink, instead of adhering to its surface. Nonetheless, it is essential to acknowledge the constraints imposed by the limited range of materials available for this bioprinting strategy in comparison to its counterparts. This limitation arises from the fact that bioinks should be suitable for cell encapsulation and provide suitable biochemical cues for the proliferation, growth, and/or differentiation of the cells. To date, the majority of the bioinks presented in the literature are hydrogel precursors, which often need to be cross-linked either during or after the scaffold fabrication [58]. The selection of the cross-linking method calls for careful experimental design to minimize potential cytotoxic or genotoxic effects. Furthermore, the bioprinting method itself could possess inherent features that could negatively affect the incorporated cells. For instance, a high shear stress in extrusion bioprinting could result in a significant decrease in cell viability, especially for bioinks with high cell densities and/or high viscosity values [106]. Nonetheless, recent studies have proposed strategies to minimize the printing-induced cell damage. For example, Pan and colleagues have proposed a nature-inspired strategy for cell protection during bioprinting using a pyrogallol-alginate cell encapsulation system, which mimics the dormant state of plant seeds when they are exposed to adverse environmental conditions [107].

Apart from the selected bioink, crosslinking mechanism, and printing approach, the selected shape-shifting stimulus should also be compatible with living cells in Strategy 3. In a recent study, Luo *et al* printed scaffolds from AA and GelMA loaded with human embryonic kidney cells, which self-transformed into saddle-like structures upon NIR irradiation [79]. The scaffolds were able to maintain their deformed structures for at least 14 d, while the printed cells retained significant viability. Overall, this approach requires a delicate parameter optimization and selection of cross-linking method and 4D stimulus. In certain cases, the complexity of the system could be reduced by opting for a stimulus inherent to bioprinting, such as physiological temperature or humidity. For instance, Ding and colleagues developed a jammed micro-flake hydrogel from ionically crosslinked OMA as a bioink for 4D bioprinting [81]. The hydrogels were crosslinked using UV light and a crosslinking gradient along the thickness direction of the scaffolds was established. Immersion of these constructs in the culture medium resulted in self-bending. Three different cell types were investigated (i.e. NIH3T3, HeLa and hMSCs) and cartilage-like tissue formation was demonstrated in bent hydrogel bars. In another study, Díaz-Payno, Kalogeropoulou *et al* 4D bioprinted a scaffold that recapitulated some aspects of the complex multilayered curved structure of articular cartilage based on differential swelling of the layers using a tyramine-HA containing AA bioink embedded with hMSCs [27].

7. Discussion and future directions

4D printing is an emerging technology that is expected to revolutionize the TERM field. 4D printing consists of 3D printing a scaffold that transforms into a distinct stable state upon the application of one or more stimuli, featuring the introduction of time as the fourth dimension (4D). In this review, we presented an overview of the recent developments in this exciting area of research that aims to enable the biofabrication of highly complex structures through the shape-change of (bio)printed constructs for TERM applications. Our findings show that the two most common mechanisms used in TERM applications are shape-memory (e.g. with such materials as PLA, PGDA, and polyurethanes) and differential swelling with different combinations of AA, HA, or gelatin (figure 7(a)). The selection of the shape transformation mechanism is closely correlated to the cell seeding strategy. For instance, in most shape-memory studies in which cells are used, they are seeded post-transformation. On the other hand, most swelling-based studies explore the addition of the cells to the material from the very beginning of the fabrication setup (figure 7(b)). Several biomedical applications have been described, but the most widely studied target tissues to date are bone, vascular, and cardiac tissues (figure 7(c)). Despite the remarkable 4D printing applications already reported, there are several challenges that are yet to overcome.

Firstly, there is a limited number of suitable inks, most of which are responsive to a single type of stimulus. However, in an environment as complex as the human body, tissues are exposed to multiple stimuli and regulatory processes. Therefore, a possible future research direction could be the use of the complexity of the human body as a mechanism to increase the capabilities of 4D printed structures. For instance, the use of multi-responsive smart materials or a combination of multiple single-responsive materials in a single structure could allow for the fabrication of scaffolds with more than two stable states, capable of performing complex functions without the need for any external stimuli. Secondly, the effects of the stimuli on the cells need to be better characterized. For instance, although light is a promising stimulus for 4D printing applications in TE, more in-depth research is required to address concerns regarding potential toxic or damaging effects of light and the photo-initiators used on the cells, as well as the risk of tissue damage caused by heat generation during photo-thermal conversion [84].

Other stimuli, already used in 4D printing, such as magnetic and electric fields, could be useful for

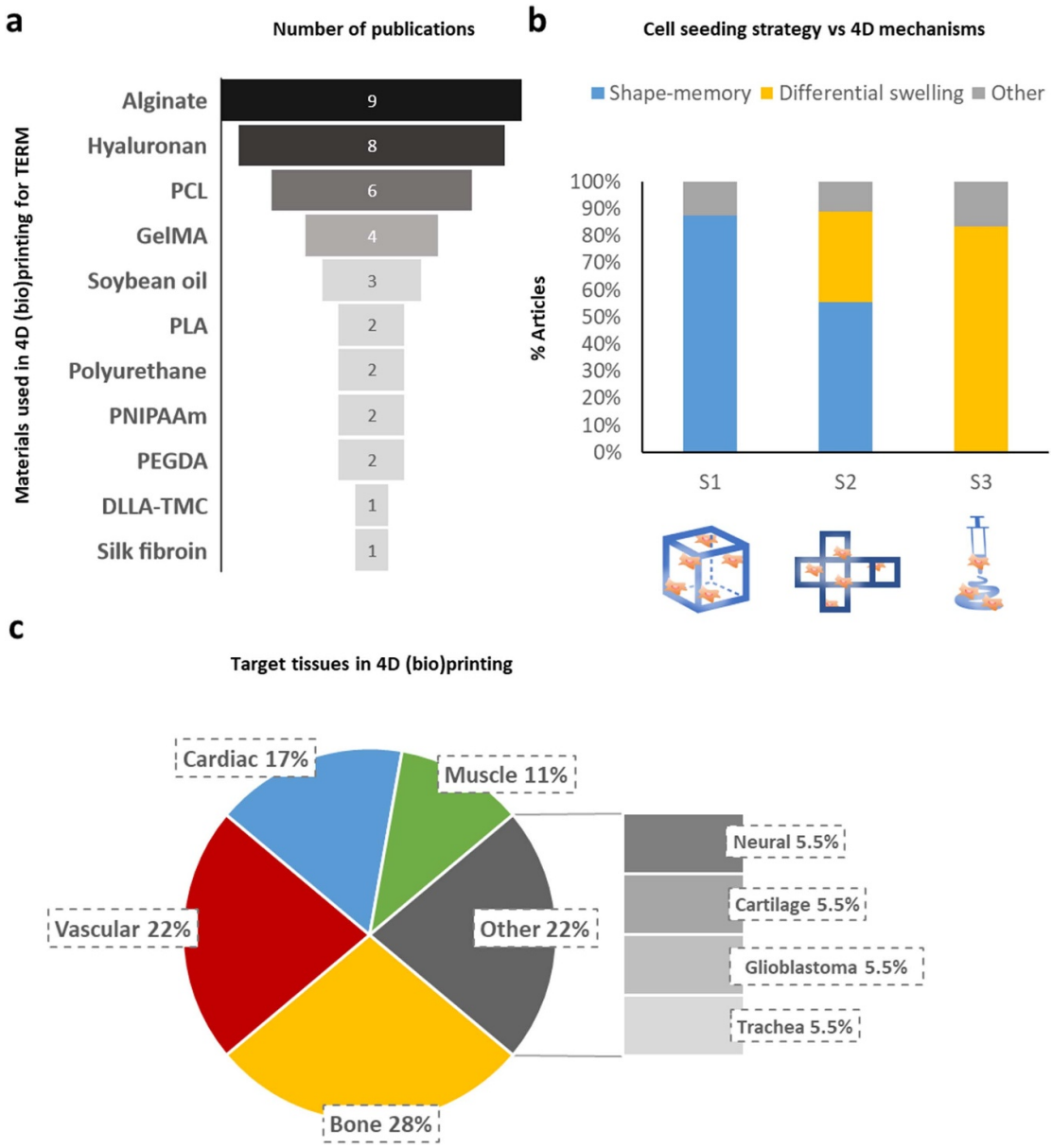

Figure 7. Biomaterials, mechanisms, and the targeted tissue of shape-based transformation 4D (bio)printing for TERM applications. (a) A list of the materials used in 4D (bio)printing research articles organized by the number of articles. (b) The percentage of the articles in which the different shape-changing mechanisms are used in each of the different seeding strategies (S1, S2, S3). (c) The target tissues in 4D (bio)printing applications.

TERM applications. The main advantages of magnetic field include the remote stimulus application as well as the ability to easily and harmlessly penetrate most materials [109]. Zakharenko *et al* developed self-rolling and unrolling tubes by combining thermo- (PCL) and magneto-responsive materials (PNIPAAm) [110] that could be used for controlled cell encapsulation and release. In another innovative 3D bioprinting approach proposed by Betsch *et al*, a conventional extrusion printer was modified by adding a magnet close to the printing bed [111], which allowed for the application of a magnetic field to the iron-containing agarose/collagen bioink during extrusion. In this way, it was possible to achieve collagen fiber alignment parallel to the direction of the applied field, producing chondrocyte-laden scaffolds that mimicked the native collagen architecture of the human articular cartilage.

The use of electric fields is particularly attractive for the fabrication of scaffolds that promote the regeneration of electrically active tissues. To date, very few attempts have been made at electrically assisted 4D printing. For instance, Cvetkovic *et al* used SLA to print hydrogel poly(ethylene glycol) diacrylate (PEGDA) 'bio-bots', powered by the contraction of engineered skeletal muscle [112]. Electric fields have also been used to direct the orientation of muscle cells. In a recent study by Yang *et al*, an electric field-assisted 3D bioprinting system was presented for the fabrication of scaffolds with a cell-alignment cue

[28]. Gelatin-based bioinks were extruded through a modified nozzle while simultaneously exposed to an external electric field to induce the alignment of the embedded myoblasts. The printed fibers were deposited on top of a patterned gelatin film that underwent self-rolling upon immersion in water, resulting in the formation of cell-laden fibrous bundles.

Thirdly, 4D bioprinting seems to be limited to extrusion and DLP-based bioprinting, but there are other fabrication techniques, such as inkjet-based bioprinting and laser-assisted bioprinting with high potential for TERM 4D applications. Inkjet bioprinting was the first printing method that was combined with cell-laden materials [113] and is based on the same working principles as conventional inkjet printing. A cell-containing hydrogel precursor is loaded in the ink cartridge, which is connected to the printing head and is ejected in droplets. The main advantages of inkjet bioprinting include high printing speed, relatively high cell viability, low cost due to the similarity of the devices to the commercially available printers as well as a relatively high printing resolution, with droplets containing one or two cells printed in $\sim$ 50 μm wide patterns [114]. However, there are several points to take into consideration when using bioinks. For example, in thermal inkjet bioprinting, the localized temperature increase, ranging from 200 °C to 300 °C, may be detrimental to cell viability and the stability of biological molecules if applied for more than $\sim$ 2 μs [20]. In addition, the bioink must be liquid to be effectively ejected from the printing head. Thus, a common issue of this technology is head-clogging due to high bioink viscosity, material drying within the printing head, or cell settling in the cartridge.

Laser-assisted bioprinting (LAB) originates from the laser-induced forward transfer technology [115]. The system consists of a focused laser pulse that causes volatilization of a liquid bioink at the donor/-bioink interface, generating a high-pressure bubble that ejects the cell-containing material toward the collector substrate. Since LAB is a non-contact printing method, both clogging and shear-induced cell damage are avoided. It is a bioprinting technology that is compatible with a moderately wide range of viscosities (1 mPa·s–300 mPa·s) and is capable of depositing high cell densities with resolutions down to a single cell per drop [116]. However, the side effects that laser exposure may have on cells are not yet fully comprehended. Additionally, LAB systems are expensive in comparison to inkjet or extrusion bioprinting and the printing procedure is complex and often requires a pre-printing preparation step which significantly increases the fabrication time [20].

Despite the several challenges of the 4D (bio)printing process, current shape-changes relying on bilayers are relatively simple. To increase the complexity of such changes and mimic natural processes of high complexity, there is a need to include dual or even multiple shape-changing mechanisms. Previously, researchers have combined 3D printing with self-folding origami to program shape-shifting of flat soft matter with several patterned surfaces [117]. Such strategies could contribute to the future developments of 4D (bio)printing.

Finally, the development of material-specific models for reliable prediction of the final shape of the scaffolds is needed. Although individual studies have tried to create databases for modeling the shape-shifting behavior of 4D printed scaffolds [65], these are based on equations that have been optimized for each particular application and conditions. Therefore, developing computational models that can be easily modified for a wide spectrum of 4D printing applications could provide a valuable tool for designing complex shape-shifting patterns, optimizing experiments as well as comparing results among different studies.

8. Conclusions

4D printing has emerged as a cutting-edge technology, enabling the fabrication of highly sophisticated scaffolds with controllable, dynamic shapes by introducing the additional dimension of time. This has marked the beginning of a new era in the field of biofabrication. This review focused on the shape-shifting aspect of 4D printing and its application in the field of TERM. We observed that the most common 4D mechanisms are based on shape-memory materials when printing without cells and is mainly limited to swelling-based differential growth when working with embedded cells. This field is still in its infancy and there is a need to develop smart biocompatible strategies that can use a wider range of 4D mechanisms, stimuli, and printing techniques.

Data availability statement

All data that support the findings of this study are included within the article (and any supplementary files).

Acknowledgments

We further gratefully acknowledge financial support by Medical Delta Programme RegMed4D and the Convergence programme Syn-Cells for Health(care) under the theme of Health and Technology.

Conflict of interest

The authors declare no conflict of interest.

ORCID iDs

Maria Kalogeropoulou https://orcid.org/0000-0002-1084-5766
Pedro J Díaz-Payno https://orcid.org/0000-0002-3744-9093
Mohammad J Mirzaali https://orcid.org/0000-0002-5349-6922
Gerjo J V M van Osch https://orcid.org/0000-0003-1852-6409
Lidy E Fratila-Apachitei https://orcid.org/0000-0002-7341-4445
Amir A Zadpoor https://orcid.org/0000-0003-3234-2112

References

[1] Thomson R C, Wake M C, Yaszemski M J and Mikos A G 1995 pp 245–74
[2] Chan B P and Leong K W 2008 Scaffolding in tissue engineering: general approaches and tissue-specific considerations *Eur. Spine J.* **17** 467
[3] Liao C J, Chen C F, Chen J H, Chiang S F, Lin Y J and Chang K Y 2002 Fabrication of porous biodegradable polymer scaffolds using a solvent merging/particulate leaching method *J. Biomed. Mater. Res.* **59** 676
[4] Poursamar S A, Hatami J, Lehner A N, da Silva C L, Ferreira F C and Antunes A P M 2015 Gelatin porous scaffolds fabricated using a modified gas foaming technique: characterisation and cytotoxicity assessment *Mater. Sci. Eng.* C **48** 63
[5] Correlo V M, Costa-Pinto A R, Sol P, Covas J A, Bhattacharya M, Neves N M and Reis R L 2010 Melt processing of chitosan–based fibers and fiber–mesh scaffolds for the engineering of connective tissues *Macromol. Biosci.* **10** 1495
[6] Allaf R M 2018 4 Melt-molding technologies for 3D scaffold engineering *Functional 3D Tissue Engineering Scaffolds: Materials, Technologies, and Applications* p 75–100
[7] Cunniffe G M *et al* 2019 Tissue-specific extracellular matrix scaffolds for the regeneration of spatially complex musculoskeletal tissues *Biomaterials* **188** 63
[8] Browe D C, Burdis R, Díaz-Payno P J, Freeman F E, Nulty J M, Buckley C T, Brama P A J and Kelly D J 2022 Promoting endogenous articular cartilage regeneration using extracellular matrix scaffolds *Mater. Today Bio* **16** 100343
[9] Sachlos E and Czernuszka J 2003 Making tissue engineering scaffolds work. Review: the application of solid freeform fabrication technology to the production of tissue engineering scaffolds *Eur. Cell. Mater.* **5** 29
[10] Liaw C-Y and Guvendiren M 2017 Current and emerging applications of 3D printing in medicine *Biofabrication* **9** 024102
[11] Chia H N and Wu B M 2015 Recent advances in 3D printing of biomaterials *J. Biol. Eng.* **9** 4
[12] Yan Q, Dong H, Su J, Han J, Song B, Wei Q and Shi Y 2018 A review of 3D printing technology for medical applications *Engineering* **4** 729
[13] Merceron T K, Burt M, Seol Y-J, Kang H-W, Lee S J, Yoo J J and Atala A 2015 A 3D bioprinted complex structure for engineering the muscle–tendon unit *Biofabrication* **7** 035003
[14] Martínez Ávila H, Schwarz S, Rotter N and Gatenholm P 2016 3D bioprinting of human chondrocyte-laden nanocellulose hydrogels for patient-specific auricular cartilage regeneration *Bioprinting* **1–2** 22
[15] Won J-Y, Park C-Y, Bae J-H, Ahn G, Kim C, Lim D-H, Cho D-W, Yun W-S, Shim J-H and Huh J-B 2016 Evaluation of 3D printed PCL/PLGA/ β -TCP versus collagen membranes for guided bone regeneration in a beagle implant model *Biomed. Mater.* **11** 055013
[16] Ng W L, Yeong W Y and Naing M W 2016 Polyelectrolyte gelatin-chitosan hydrogel optimized for 3D bioprinting in skin tissue engineering *Int. J. Bioprint.* **2** 53–62
[17] Jia W *et al* 2016 Direct 3D bioprinting of perfusable vascular constructs using a blend bioink *Biomaterials* **106** 58
[18] Tse C, Whiteley R, Yu T, Stringer J, MacNeil S, Haycock J W and Smith P J 2016 Inkjet printing Schwann cells and neuronal analogue NG108-15 cells *Biofabrication* **8** 015017
[19] Giannopoulos A A, Mitsouras D, Yoo S-J, Liu P P, Chatzizisis Y S and Rybicki F J 2016 Applications of 3D printing in cardiovascular diseases *Nat. Rev. Cardiol.* **13** 701
[20] Murphy S V and Atala A 2014 3D bioprinting of tissues and organs *Nat. Biotechnol.* **32** 773
[21] Park J H, Hong J M, Ju Y M, Jung J W, Kang H-W, Lee S J, Yoo J J, Kim S W, Kim S H and Cho D-W 2015 A novel tissue-engineered trachea with a mechanical behavior similar to native trachea *Biomaterials* **62** 106
[22] Richards D, Jia J, Yost M, Markwald R and Mei Y 2017 3D bioprinting for vascularized tissue fabrication *Ann. Biomed. Eng.* **45** 132
[23] Tibbits S 2014 4D printing: multi–material shape change *Archit. Des.* **84** 116
[24] Sydney Gladman A, Matsumoto E A, Nuzzo R G, Mahadevan L and Lewis J A 2016 Biomimetic 4D printing *Nat. Mater.* **15** 413
[25] Miao S, Cui H, Nowicki M, Xia L, Zhou X, Lee S, Zhu W, Sarkar K, Zhang Z and Zhang L G 2018 Stereolithographic 4D bioprinting of multiresponsive architectures for neural engineering *Adv. Biosyst.* **2** 1800101
[26] Naficy S, Gately R, Gorkin R, Xin H and Spinks G M 2017 4D printing of reversible shape morphing hydrogel structures *Macromol. Mater. Eng.* **302** 1600212
[27] Díaz-Payno P J, Kalogeropoulou M, Muntz I, Kingma E, Kops N, D'Este M, Koenderink G H, Fratila-Apachitei L E, van Osch G J V M and Zadpoor A A 2023 Swelling–dependent shape–based transformation of a human mesenchymal stromal cells–laden 4D bioprinted construct for cartilage tissue engineering *Adv. Healthc. Mater.* **12** 2201891
[28] Yang G H, Kim W, Kim J and Kim G 2021 A skeleton muscle model using GelMA-based cell-aligned bioink processed with an electric-field assisted 3D/4D bioprinting *Theranostics* **11** 48
[29] Wang C *et al* 2020 Advanced reconfigurable scaffolds fabricated by 4D printing for treating critical-size bone defects of irregular shapes *Biofabrication* **12** 045025
[30] Choi J, Kwon O-C, Jo W, Lee H J and Moon M-W 2015 4D printing technology: a review *3D Print Addit Manuf.* **2** 159
[31] Gao B, Yang Q, Zhao X, Jin G, Ma Y and Xu F 2016 4D bioprinting for biomedical applications *Trends Biotechnol.* **34** 746
[32] Aronsson C, Jury M, Naeimipour S, Boroojeni F R, Christoffersson J, Lifwergren P, Mandenius C-F, Selegård R and Aili D 2020 Dynamic peptide-folding mediated biofunctionalization and modulation of hydrogels for 4D bioprinting *Biofabrication* **12** 035031
[33] Mandon C, Blum L and Marquette C 2017 3D–4D printed objects: new bioactive material opportunities *Micromachines* **8** 102
[34] Li Y-C, Zhang Y S, Akpek A, Shin S R and Khademhosseini A 2016 4D bioprinting: the

next-generation technology for biofabrication enabled by stimuli-responsive materials *Biofabrication* **9** 012001
[35] Yang Q, Gao B and Xu F 2020 Recent advances in 4D bioprinting *Biotechnol. J.* **15** 1900086
[36] Scott Crump S 1989 *Apparatus and Method for Creating Three-Dimensional Objects* US5121329A (available at: https://patents.google.com/patent/US5121329A/en)
[37] Wu G-H and Hsu S 2015 Review: polymeric-based 3D printing for tissue engineering *J. Med. Biol. Eng.* **35** 285
[38] Hendrikson W J, Rouwkema J, Clementi F, van Blitterswijk C A, Farè S and Moroni L 2017 Towards 4D printed scaffolds for tissue engineering: exploiting 3D shape memory polymers to deliver time-controlled stimulus on cultured cells *Biofabrication* **9** 031001
[39] Miao S, Zhu W, Castro N J, Leng J and Zhang L G 2016 Four-dimensional printing hierarchy scaffolds with highly biocompatible smart polymers for tissue engineering applications *Tissue Eng.* C **22** 952–63
[40] Senatov F S, Niaza K V, Zadorozhnyy M Y, Maksimkin A V, Kaloshkin S D and Estrin Y Z 2016 Mechanical properties and shape memory effect of 3D-printed PLA-based porous scaffolds *J. Mech. Behav. Biomed. Mater.* **57** 139
[41] Senatov F S, Zadorozhnyy M Y, Niaza K V, Medvedev V V, Kaloshkin S D, Anisimova N Y, Kiselevskiy M V and Yang K-C 2017 Shape memory effect in 3D-printed scaffolds for self-fitting implants *Eur. Polym. J.* **93** 222
[42] Tan Z, Parisi C, Di Silvio L, Dini D and Forte A E 2017 Cryogenic 3D printing of super Soft hydrogels *Sci. Rep.* **7** 16293
[43] Adamkiewicz M and Rubinsky B 2015 Cryogenic 3D printing for tissue engineering *Cryobiology* **71** 518
[44] Lewis J A 2006 Direct ink writing of 3D functional materials *Adv. Funct. Mater.* **16** 2193
[45] Lewis J A and Gratson G M 2004 Direct writing in three dimensions *Mater. Today* **7** 32
[46] Abshirini M, Marashizadeh P, Saha M C, Altan M C and Liu Y 2022 Three-dimensional printed highly porous and flexible conductive polymer nanocomposites with dual-scale porosity and piezoresistive sensing functions *ACS Appl. Mater. Interfaces* **15** 14810–25
[47] Bakarich S E, Gorkin R, In het Panhuis M and Spinks G M 2015 4D printing with mechanically robust, thermally actuating hydrogels *Macromol. Rapid Commun.* **36** 1211
[48] Kim H, Kim J, Koo J, Lee J, Kim H J and Hyun J 2023 Embedded direct ink writing 3D printing of UV curable resin/sepiolite composites with nano orientation *ACS Omega* 23554–65
[49] Putra N E *et al* 2023 Extrusion-based 3D printing of biodegradable, osteogenic, paramagnetic, and porous FeMn-akermanite bone substitutes *Acta Biomater.* **162** 182
[50] Zhao Y, Zhu J, He W, Liu Y, Sang X and Liu R 2023 The splanchnic mesenchyme is the tissue of origin for pancreatic fibroblasts during homeostasis and tumorigenesis *Nat. Commun.* **14** 1
[51] Kuang X, Chen K, Dunn C K, Wu J, Li V C F and Qi H J 2018 3D printing of highly stretchable, shape-memory, and self-healing elastomer toward novel 4D printing *ACS Appl. Mater. Interfaces* **10** 7381
[52] Wang Y, Miao Y, Zhang J, Wu J P, Kirk T B, Xu J, Ma D and Xue W 2018 Three-dimensional printing of shape memory hydrogels with internal structure for drug delivery *Mater. Sci. Eng.* C **84** 44
[53] Knowlton S, Anand S, Shah T and Tasoglu S 2018 Bioprinting for neural tissue engineering *Trends Neurosci.* **41** 31
[54] Park J Y, Choi J-C, Shim J-H, Lee J-S, Park H, Kim S W, Doh J and Cho D-W 2014 A comparative study on collagen type I and hyaluronic acid dependent cell behavior for osteochondral tissue bioprinting *Biofabrication* **6** 035004
[55] Owens C M, Marga F, Forgacs G and Heesch C M 2013 Biofabrication and testing of a fully cellular nerve graft *Biofabrication* **5** 045007
[56] Mandrycky C, Wang Z, Kim K and Kim D-H 2016 3D bioprinting for engineering complex tissues *Biotechnol. Adv.* **34** 422
[57] Khalil S and Sun W 2007 Biopolymer deposition for freeform fabrication of hydrogel tissue constructs *Mater. Sci. Eng.* C **27** 469
[58] Schwab A, Levato R, D'Este M, Piluso S, Eglin D and Malda J 2020 Printability and shape fidelity of bioinks in 3D bioprinting *Chem. Rev.* **120** 11028
[59] Paxton N, Smolan W, Böck T, Melchels F, Groll J and Jungst T 2017 Proposal to assess printability of bioinks for extrusion-based bioprinting and evaluation of rheological properties governing bioprintability *Biofabrication* **9** 044107
[60] Kirillova A, Maxson R, Stoychev G, Gomillion C T and Ionov L 2017 4D biofabrication using shape–morphing hydrogels *Adv. Mater.* **29** 1703443
[61] Miao S, Zhu W, Castro N J, Nowicki M, Zhou X, Cui H, Fisher J P and Zhang L G 2016 4D printing smart biomedical scaffolds with novel soybean oil epoxidized acrylate *Sci. Rep.* **6** 27226
[62] Miao S, Nowicki M, Cui H, Lee S-J, Zhou X, Mills D K and Zhang L G 2019 4D anisotropic skeletal muscle tissue constructs fabricated by staircase effect strategy *Biofabrication* **11** 035030
[63] Stansbury J W and Idacavage M J 2016 3D printing with polymers: challenges among expanding options and opportunities *Dent. Mater.* **32** 54
[64] Weems A C, Arno M C, Yu W, Huckstepp R T R and Dove A P 2021 4D polycarbonates via stereolithography as scaffolds for soft tissue repair *Nat. Commun.* **12** 3771
[65] Kim S H *et al* 2020 4D-bioprinted silk hydrogels for tissue engineering *Biomaterials* **260** 120281
[66] Loewner S, Heene S, Baroth T, Heymann H, Cholewa F, Blume H and Blume C 2022 Recent advances in melt electro writing for tissue engineering for 3D printing of microporous scaffolds for tissue engineering *Front. Bioeng. Biotechnol.* **10** 896719
[67] Constante G, Apsite I, Alkhamis H, Dulle M, Schwarzer M, Caspari A, Synytska A, Salehi S and Ionov L 2021 4D biofabrication using a combination of 3D printing and melt-electrowriting of shape-morphing polymers *ACS Appl. Mater. Interfaces* **13** 12767
[68] Apsite I, Constante G, Dulle M, Vogt L, Caspari A, Boccaccini A R, Synytska A, Salehi S and Ionov L 2020 4D Biofabrication of fibrous artificial nerve graft for neuron regeneration *Biofabrication* **12** 035027
[69] Apsite I, Uribe J M, Posada A F, Rosenfeldt S, Salehi S and Ionov L 2020 4D biofabrication of skeletal muscle microtissues *Biofabrication* **12** 015016
[70] Shirazi S F S, Gharehkhani S, Mehrali M, Yarmand H, Metselaar H S C, Adib Kadri N and Osman N A A 2015 A review on powder-based additive manufacturing for tissue engineering: selective laser sintering and inkjet 3D printing *Sci. Technol. Adv. Mater.* **16** 033502
[71] Cui C, Kim D-O, Pack M Y, Han B, Han L, Sun Y and Han L-H 2020 4D printing of self-folding and cell-encapsulating 3D microstructures as scaffolds for tissue-engineering applications *Biofabrication* **12** 045018
[72] Booth M J, Restrepo Schild V, Box S J and Bayley H 2017 Light-patterning of synthetic tissues with single droplet resolution *Sci. Rep.* **7** 9315
[73] Miao S, Zhu W, Castro N J, Leng J and Zhang L G 2016 Four-dimensional printing hierarchy scaffolds with highly biocompatible smart polymers for tissue engineering applications *Tissue Eng.* C **22** 952
[74] Foresti R, Rossi S and Selleri S 2019 *2019 IEEE Int. Conf. on BioPhotonics (Biophotonics)* (IEEE) pp 1–2
[75] Zhang C, Cai D, Liao P, Su J-W, Deng H, Vardhanabhuti B, Ulery B D, Chen S-Y and Lin J 2021 4D printing of shape-memory polymeric scaffolds for adaptive biomedical implantation *Acta Biomater.* **122** 101

[76] Chadwick M, Yang C, Liu L, Gamboa C M, Jara K, Lee H and Sabaawy H E 2020 Rapid processing and drug evaluation in glioblastoma patient-derived organoid models with 4D bioprinted arrays *iScience* **23** 101365
[77] Zarek M, Mansour N, Shapira S and Cohn D 2017 4D printing of shape memory–based personalized endoluminal medical devices *Macromol. Rapid Commun.* **38** 1600628
[78] Wang Y, Cui H, Wang Y, Xu C, Esworthy T J, Hann S Y, Boehm M, Shen Y-L, Mei D and Zhang L G 2021 4D printed cardiac construct with aligned myofibers and adjustable curvature for myocardial regeneration *ACS Appl. Mater. Interfaces* **13** 12746
[79] Luo Y, Lin X, Chen B and Wei X 2019 Cell-laden four-dimensional bioprinting using near-infrared-triggered shape-morphing alginate/polydopamine bioinks *Biofabrication* **11** 045019
[80] Ding A, Lee S J, Ayyagari S, Tang R, Huynh C T and Alsberg E 2022 4D biofabrication via instantly generated graded hydrogel scaffolds. *Bioact. Mater.* **7** 324
[81] Ding A, Jeon O, Cleveland D, Gasvoda K L, Wells D, Lee S J and Alsberg E 2022 Jammed micro-flake hydrogel for four-dimensional living cell bioprinting *Adv. Mater.* **34** 2109394
[82] Gugulothu S B and Chatterjee K 2023 Visible light-based 4D-bioprinted tissue scaffold *ACS Macro Lett.* **12** 494
[83] Evangelista D, Hotton S and Dumais J 2011 The mechanics of explosive dispersal and self-burial in the seeds of the filaree, Erodium cicutarium (Geraniaceae) *J. Exp. Biol.* **214** 521
[84] Reyssat E and Mahadevan L 2009 Hygromorphs: from pine cones to biomimetic bilayers *J. R. Soc. Interface* **6** 951
[85] Han D, Lu Z, Chester S A and Lee H 2018 Micro 3D printing of a temperature-responsive hydrogel using projection micro-stereolithography *Sci. Rep.* **8** 1963
[86] Jiang Z, Tan M L, Taheri M, Yan Q, Tsuzuki T, Gardiner M G, Diggle B and Connal L A 2020 Strong, self–healable, and recyclable visible–light–responsive hydrogel actuators *Angew. Chem., Int. Ed.* **59** 7049
[87] Kashyap D, Kishore Kumar P and Kanagaraj S 2018 4D printed porous radiopaque shape memory polyurethane for endovascular embolization *Addit. Manuf.* **24** 687
[88] Melocchi A *et al* 2019 Expandable drug delivery system for gastric retention based on shape memory polymers: development via 4D printing and extrusion *Int. J. Pharm.* **571** 118700
[89] Apsite I, Stoychev G, Zhang W, Jehnichen D, Xie J and Ionov L 2017 Porous stimuli-responsive self-folding electrospun mats for 4D biofabrication *Biomacromolecules* **18** 3178
[90] Doberenz F, Zeng K, Willems C, Zhang K and Groth T 2020 Thermoresponsive polymers and their biomedical application in tissue engineering—a review *J. Mater. Chem.* B **8** 607
[91] Tiwari A P, Bhattarai D P, Maharjan B, Ko S W, Kim H Y, Park C H and Kim C S 2019 Polydopamine-based implantable multifunctional nanocarpet for highly efficient photothermal–chemo therapy *Sci. Rep.* **9** 2943
[92] Lendlein A and Kelch S 2002 Shape–memory polymers *Angew. Chem., Int. Ed.* **41** 2034
[93] Huang W M, Yang B, An L, Li C and Chan Y S 2005 Water-driven programmable polyurethane shape memory polymer: demonstration and mechanism *Appl. Phys. Lett.* **86** 114105
[94] Lendlein A, Jiang H, Jünger O and Langer R 2005 Light-induced shape-memory polymers *Nature* **434** 879
[95] Mohr R, Kratz K, Weigel T, Lucka-Gabor M, Moneke M and Lendlein A 2006 Initiation of shape-memory effect by inductive heating of magnetic nanoparticles in thermoplastic polymers *Proc. Natl Acad. Sci.* **103** 3540
[96] Wei Z G, Sandstroröm R and Miyazaki S 1998 Shape-memory materials and hybrid composites for smart systems: Part I Shape-memory materials *J. Mater. Sci.* **33** 3743
[97] Liu Y, Gall K, Dunn M L and McCluskey P 2004 Thermomechanics of shape memory polymer nanocomposites *Mech. Mater.* **36** 929
[98] Ratna D and Karger-Kocsis J 2008 Recent advances in shape memory polymers and composites: a review *J. Mater. Sci.* **43** 254
[99] Lu H, Wu B, Yang X, Zhang J, Jian Y, Yan H, Zhang D, Xue Q and Chen T 2020 Actuating supramolecular shape memorized hydrogel toward programmable shape deformation *Small* **16** 2005461
[100] Wu Y, Hao X, Xiao R, Lin J, Wu Z L, Yin J and Qian J 2019 Controllable bending of bi-hydrogel strips with differential swelling *Acta Mech. Solida Sin.* **32** 652
[101] Timoshenko S 1925 Analysis of bi-metal thermostats *J. Opt. Soc. Am.* **11** 233
[102] Pyo Y, Kang M, Young Jang J, Park Y, Son Y H, Choi M C, Wan Ha J, Chang Y W and Lee C S 2018 Development of vector hydrophone using thickness–shear mode piezoelectric single crystal accelerometer *Sens. Actuators* A **283** 187
[103] Kiratitanaporn W, Berry D B, Mudla A, Fried T, Lao A, Yu C, Hao N, Ward S R and Chen S 2022 3D printing a biocompatible elastomer for modeling muscle regeneration after volumetric muscle loss *Biomater. Adv.* **142** 213171
[104] Lawrence K P, Douki T, Sarkany R P E, Acker S, Herzog B and Young A R 2018 The UV/visible radiation boundary region (385–405 nm) damages skin cells and induces "dark" cyclobutane pyrimidine dimers in human skin in vivo *Sci. Rep.* **8** 1–12
[105] Gonzalez-Fernandez T, Sikorski P and Leach J K 2019 Bio-instructive materials for musculoskeletal regeneration *Acta Biomater.* **96** 20
[106] Boularaoui S, Al Hussein G, Khan K A, Christoforou N and Stefanini C 2020 An overview of extrusion-based bioprinting with a focus on induced shear stress and its effect on cell viability *Bioprinting* **20** e00093
[107] Pan H M, Chen S, Jang T S, Han W T, Do Jung H, Li Y and Song J 2019 Plant seed-inspired cell protection, dormancy, and growth for large-scale biofabrication *Biofabrication* **11** 025008
[108] Miao S *et al* 2018 Photolithographic-stereolithographic-tandem fabrication of 4D smart scaffolds for improved stem cell cardiomyogenic differentiation *Biofabrication* **10** 035007
[109] Peters C, Hoop M, Pané S, Nelson B J and Hierold C 2016 Degradable magnetic composites for minimally invasive interventions: device fabrication, targeted drug delivery, and cytotoxicity tests *Adv. Mater.* **28** 533
[110] Zakharchenko S, Puretskiy N, Stoychev G, Stamm M and Ionov L 2010 Temperature controlled encapsulation and release using partially biodegradable thermo-magneto-sensitive self-rolling tubes *Soft Matter* **6** 2633
[111] Betsch M, Cristian C, Lin Y-Y, Blaeser A, Schöneberg J, Vogt M, Buhl E M, Fischer H and Duarte Campos D F 2018 Incorporating 4D into bioprinting: real-time magnetically directed collagen fiber alignment for generating complex multilayered tissues *Adv. Healthc. Mater.* **7** 1800894
[112] Cvetkovic C, Raman R, Chan V, Williams B J, Tolish M, Bajaj P, Sakar M S, Asada H H, Saif M T A and Bashir R 2014 Three-dimensionally printed biological machines powered by skeletal muscle *Proc. Natl Acad. Sci.* **111** 10125
[113] Xu T, Petridou S, Lee E H, Roth E A, Vyavahare N R, Hickman J J and Boland T 2004 Construction of high-density bacterial colony arrays and patterns by the ink-jet method *Biotechnol. Bioeng.* **85** 29
[114] Nakamura M, Kobayashi A, Takagi F, Watanabe A, Hiruma Y, Ohuchi K, Iwasaki Y, Horie M, Morita I and

Takatani S 2005 Biocompatible inkjet printing technique for designed seeding of individual living cells *Tissue Eng.* **11** 1658

[115] Barron J A, Ringeisen B R, Kim H, Spargo B J and Chrisey D B 2004 Application of laser printing to mammalian cells *Thin Solid Films* **453–454** 383

[116] Guillotin B *et al* 2010 Laser assisted bioprinting of engineered tissue with high cell density and microscale organization *Biomaterials* **31** 7250

[117] van Manen T, Janbaz S and Zadpoor A A 2018 Programming the shape-shifting of flat soft matter *Mater. Today* **21** 144